

Composition and temperature dependence of cation ordering in Ni-Mg olivine solid solutions: a time-of-flight neutron powder diffraction and EXAFS study

C. MICHAEL B. HENDERSON,^{1,*} SIMON A.T. REDFERN,² RONALD I. SMITH,³ KEVIN S. KNIGHT,³ AND JOHN M. CHARNOCK¹

¹Department of Earth Sciences, University of Manchester, Manchester M13 9PL, U.K. and Daresbury Laboratory, CLRC, Warrington WA4 4AD, U.K.

²Department of Earth Sciences, Downing Street, University of Cambridge, Cambridge CB2 3EQ, U.K.

³ISIS, Rutherford Appleton Laboratory, CLRC, Chilton, Oxfordshire OX11 0QX, U.K.

ABSTRACT

The non-convergent ordering of Mg and Ni over the M1 and M2 sites of synthetic olivines has been studied using “time of flight” neutron powder diffraction and X-ray absorption spectroscopy (EXAFS). The compositional dependence of order/disorder at room temperature was established for solid solutions of general formula $(\text{Mg}_{1-x}\text{Ni}_x)_2\text{SiO}_4$, where $X = 0.15, 0.2, 0.25, 0.3, 0.5,$ and 0.8 atoms Ni (X_{Ni} ; i.e., mole fraction of Ni-olivine end-member). Ni orders into M1 with $K_D = (\text{Ni}/\text{Mg in M1})/(\text{Ni}/\text{Mg in M2})$ reaching a maximum of 9.5 at a composition of $\text{Mg}_{1.6}\text{Ni}_{0.4}\text{SiO}_4$. The temperature dependence of order/disorder at up to 1100 °C was determined for two samples ($X_{\text{Ni}} = 0.2$ and 0.5). Between about 600 and 750 °C the samples show an *increase* in order due to kinetic effects, while above 750 °C the samples show a progressive *decrease* in order and describe an equilibrium disordering path. Equilibrium data define a Ni-Mg, M1-M2 intersite exchange energy of 21.5 ± 1.9 kJ/mol. On cooling, the blocking temperature for cation exchange is about 800 °C.

The kinetics of disordering behavior were analyzed using a Ginzburg-Landau model giving activation energies for Mg-Ni exchange between M1 and M2 for samples of composition $\text{Mg}_{1.6}\text{Ni}_{0.4}\text{SiO}_4$ and $\text{Mg}_{1.0}\text{Ni}_{1.0}\text{SiO}_4$ of 145 ± 5 and 160 ± 5 kJ/mol, respectively. The model also shows that the characteristic time scale for re-equilibration of M1-M2 order decreases from around 2.5 s at 1000° to 0.03 s at 1300 °C. This points to the inapplicability of intracrystalline Ni-Mg partitioning for obtaining geothermometry and geospeedometry information for magmatic conditions. Ni *K*-edge EXAFS data show that samples with $X_{\text{Ni}} = 0.15, 0.2, 0.25$ and 0.3 all show Ni clustering on adjacent M1 sites, indicating the presence of domains of Ni-rich and Mg-rich regions on a nanolength scale of < 10 Å. These “precipitates” are at least an order of magnitude too small to be detectable by neutron powder diffraction. We suggest that the elastic strain at the interfaces between the Ni-rich precipitates and the Mg-rich matrix is responsible for the plateau or possible maximum in the *b* unit-cell parameter as a function of composition across the solid solution, which is observed at a composition of $\text{Mg}_{1.6}\text{Ni}_{0.4}\text{SiO}_4$ at room temperature. Comparison of our data with earlier studies at high *P* and *T* on $\text{Mg}_{1.0}\text{Ni}_{1.0}\text{SiO}_4$ olivine suggests that the effect of *P* is to increase the degree of order of Ni into M1 and to slow down the kinetics of intersite exchange with a $\Delta V_{\text{disorder}}$ of 0.039 J/bar.

INTRODUCTION

Olivine (M_2SiO_4 , where M normally consists of major Mg and Fe^{2+} and minor Ni, Mn, and Ca) is common in crustal ultramafic and mafic igneous rocks and is the most abundant mineral in the Earth’s upper mantle down to depths of about 410 km; at about this depth it is believed to transform to a more dense spinel phase causing a marked seismic discontinuity (Ringwood and Major 1966). M cations occupy the two non-equivalent octahedral cation sites M1 (the smaller and more

distorted site) and M2 (the larger, less distorted site). A knowledge of the effects of composition, temperature and pressure on the non-convergent, intersite ordering/disordering of divalent cations between the M1 and M2 sites is essential if the thermodynamic, petrological and geophysical relations of this important rock-forming mineral are to be fully understood. Initial attempts to determine the temperature dependence of partitioning involved study of quenched samples at ambient conditions, mainly in the Mg- Fe^{2+} (e.g., Princivalle 1990; Ottonello et al. 1990) and Mg-Mn (Akamatsu et al. 1988) olivine systems, and contradictory data were obtained, presumably due to M1-M2 re-equilibration having occurred during quench-

* E-mail: chenderson@fs1.ge.man.ac.uk

ing. Thus, it has been shown that Mg-Fe intersite re-ordering on cooling occurs on a timescale of about 10 ms, and that blocking temperatures appear to be 500–800 °C, depending on the cooling rate (Aikawa et al. 1985). It is clear that normal experimental quenching rates from high T are too slow to freeze-in the equilibrium cation ordering, and hence in situ experiments are required for studying ordering in such mineral systems in a systematic way. In earlier studies we have used powder neutron diffraction techniques to determine the T -dependence of intersite order/disorder for synthetic FeMnSiO_4 , MgMnSiO_4 (Henderson et al. 1996; Redfern et al. 1996, 1997), FeMgSiO_4 (Redfern et al., 2000), and of the composition dependence for Fe-Mn olivine solid solutions (Redfern et al. 1998). Redfern et al. (1996) also considered the possible application of M1-M2 site disorder to assessing the cooling rates of olivine-bearing rocks (“geo-speedometry”).

Although nickel-rich olivine (liebenbergite) does occur naturally (de Waal and Calk 1973) it is something of a mineralogical curiosity. However, amongst the minor and trace element components of magmatic olivines, Ni has proved to be an extremely useful indicator of fractionation of olivine at the early stages of differentiation of basaltic magmas because of its very large olivine/liquid distribution coefficient (e.g., Henderson and Dale 1969). In addition, Hakli and Wright (1967) used quenched samples from the Makaopuhi lava lake, Hawaii, to calibrate a geothermometer based on the distribution of Ni between olivine and augite. These types of studies pointed to the need to calibrate the dependence of crystal/melt distribution coefficients as a function of composition, T , and P leading to several experimental investigations at elevated T (e.g., Leeman and Lindstrom 1978; Mysen 1979, 1982; Drake and Holloway 1981). While these studies confirmed the very high crystal/melt distribution coefficients for Ni in olivine, there was substantial disagreement regarding the concentration range over which Ni showed true Henry's Law behavior (i.e., constant distribution coefficients). Thus Mysen (1979) suggested that Henry's Law was obeyed for up to 1000 ppm Ni in olivine [e.g., $D_{\text{Ni}}(\text{ol}/\text{melt}) \sim 17$] but D values decreased at higher concentrations. In contrast, other workers showed essentially constant D values up to 6 wt% Ni (Drake and Holloway 1981) and possibly even as high as 15–20 wt% Ni (Leeman and Lindstrom 1978) in olivine. Bish (1981) and Mysen (1982) attempted to account for the systematics of Ni olivine/melt distribution in terms of cation ordering over the M1 and M2 sites.

In this paper we report the results of time-of-flight, neutron powder diffraction structural data, obtained at ATP, to assess the composition dependence of non-convergent ordering of octahedral cations in synthetic olivines of composition $(\text{Mg}_{1-x}\text{Ni}_x)_2\text{SiO}_4$ with X_{Ni} (i.e., mole fractions of Ni-olivine end-member) = 0.15, 0.20, 0.25, 0.30, 0.50, 0.80. Two of these samples ($X_{\text{Ni}} = 0.20$ and 0.50) have also been studied at temperatures up to 1100 °C to obtain information on the T -dependence of ordering. We will assess the implications of these intracrystalline ordering determinations to olivine crystal chemistry in general, and their application to the consideration of thermodynamic relations, geothermometry, geo-speedometry, and minor/trace element distribution controls.

OCTAHEDRAL CATION ORDERING IN NI-BEARING OLIVINE

Redfern et al. (1997) reviewed the earlier experimental work on divalent cation ordering in olivines, including both ex situ structural studies carried out on quenched samples, and in situ characterization at elevated T . In this paper we will restrict our literature review to the Ni-bearing system but note that most earlier studies have involved synthetic samples which were structurally characterized after quenching to room T and P .

Matsui and Syono (1968) reported that Mg-Ni olivine solid solutions have unit-cell parameters which show significant departures from Vegard's Law with a positive excess volume of mixing, largely controlled by the b unit-cell parameter values; a possible maximum occurs in the region 10–20 mol% Ni_2SiO_4 (Fig. 1). Vokurka and Rieder (1987) reported even larger positive excess molar volumes than those of Matsui and Syono. Although Rajamani et al. (1975) reported that a sample containing 51% Ni_2SiO_4 had a smaller excess volume than that indicated by the trend of Matsui and Syono (1968), unit-cell parameters for a series of samples synthesized by Boström (1987) subsequently confirmed the results of Matsui and Syono. Single crystal X-ray (Rajamani et al. 1975; Bish 1981; Boström 1987; Ottonello et al. 1989; Tsukimura and Sasaki 2000), high-pressure powder X-ray diffraction (Chen et al. 1996), crystal field spectroscopic (Wood 1974; Rager et al. 1988; Hu et al. 1990), and EXAFS investigations (Galoisy et al. 1995) all show that Ni is ordered into the smaller, more distorted M1 site. X-ray and Mössbauer work (Nord et al. 1982; Annersten et al. 1982) show that Ni is also ordered into M1 in synthetic Mg-Fe-Ni and Ni-Fe olivines.

The X-ray single crystal structure refinements of M1 and M2 site occupancies in Ni-Mg olivines and the distribution coefficients $K_D = (\text{Ni}/\text{Mg in M1})/(\text{Ni}/\text{Mg in M2})$ so derived are particularly significant in the present work. Thus, Rajamani et al. (1975) studied a sample of composition $\text{Ni}_{1.03}\text{Mg}_{0.97}\text{SiO}_4$ quenched from 1280 °C and found that $K_D = 9.2$. Bish (1981) reported that a natural liebenbergite contained only Ni in M1 while a synthetic sample of composition $\text{Ni}_{1.16}\text{Mg}_{0.84}\text{SiO}_4$ crystallized hydrothermally at 500 °C had $K_D = 9.9$. Bish used these results to consider the effect that strong ordering of Ni into M1 would have on Ni partitioning between olivine and magma (believed to be responsible for non-Henry's Law behavior), and to discuss activity – composition relations in Ni-bearing olivines. Boström (1987) studied five single crystals of Ni-Mg olivine solid solutions grown from a flux at 900 °C and found K_D values in the range 16.9 to 9.5 with higher values for more Mg-rich solid solutions. Clearly the K_D coefficients measured at room T and P do not represent equilibrium values and must depend to some degree on rates of cooling from the synthesis conditions. Indeed, it seems likely that different samples in a given solid solution series might have different degrees of intersite order. Boström (1989) addressed this problem by annealing three of his samples ($X_{\text{Ni}} = 0.30, 0.51, 0.76$) at 1300 °C followed by quenching in iced water in < 5 s. These samples were more disordered than the original, slower cooled equivalents but showed a much smaller range in K_D from 6.5 to 4.8 and thus little compositional dependence. In further work on

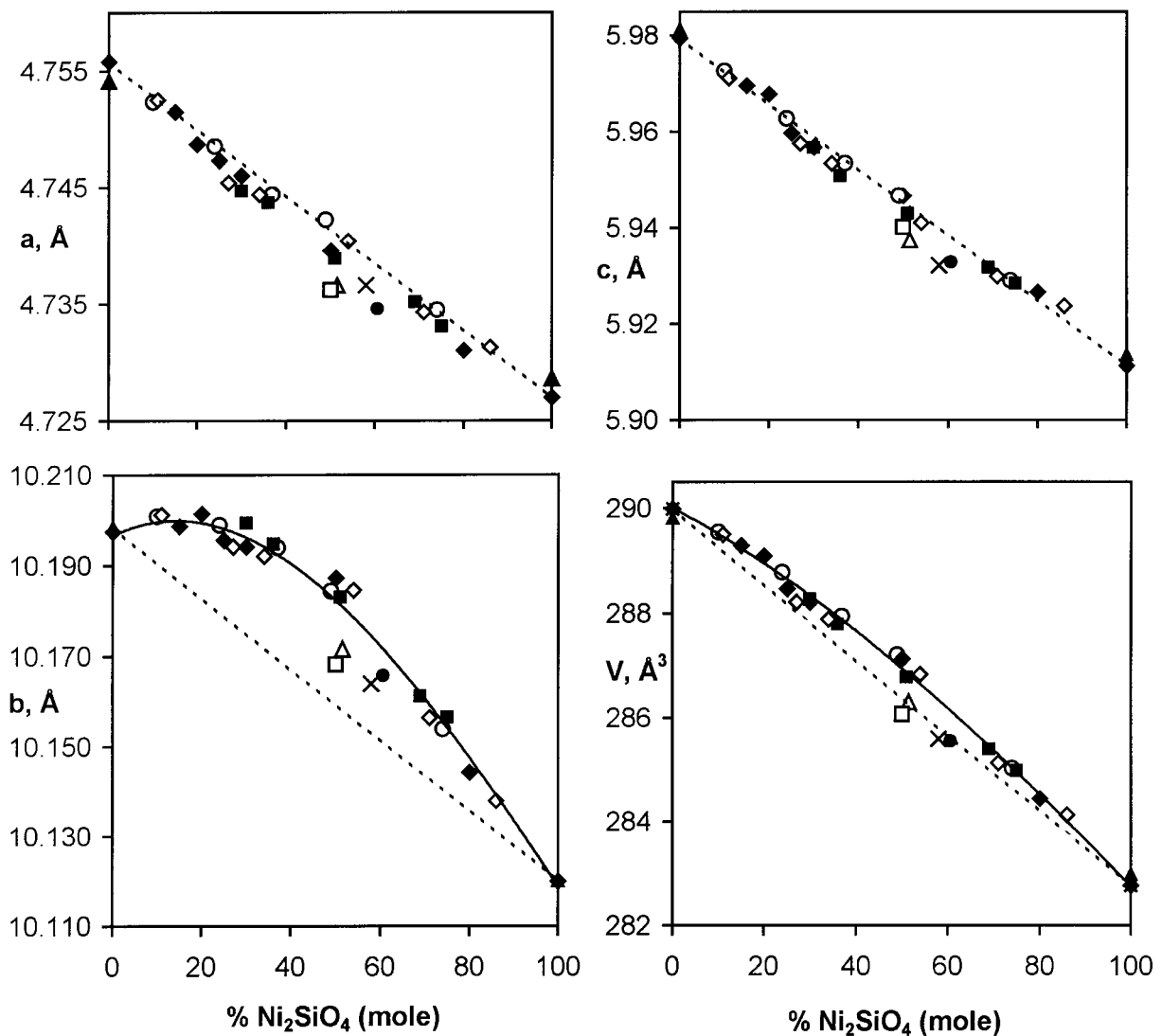


FIGURE 1. Room temperature unit-cell parameters for Ni-Mg olivine solid solutions vs. bulk composition compared with literature values. For our data 1 σ error bars are about the same size as the symbols for b , and for a , c , and V are smaller than the symbol size. Note the positive volumes of mixing and the possible maximum in the b unit-cell parameter trend at a composition close to $\text{Mg}_{1.6}\text{Ni}_{0.4}\text{SiO}_4$. Symbols: \blacklozenge this paper; \blacktriangle end-member averages (sources: Matsui and Syono, 1968; Hazen 1976; Brown, 1982; Fujino et al., 1981; Boström 1987; Della Giusta et al. 1990; Cernik et al. 1990); \circ Matsui and Syono (1968); \blacksquare Boström (1987); \diamond Hirschmann (1992); \square Chen et al. (1996); \times Bish (1981); \triangle Rajamani et al. (1975); \bullet Snyder (1993). Dashed lines join our data for the end-members, while the curved solid lines are guides to the eye fitted to our data for the solid solutions.

samples supplied by Boström, Ottonello et al. (1989) carried out annealing experiments at temperatures from 800 to 1300 °C followed by very rapid quenching (to 500 °C in about 0.5 seconds). K_D values at room T and P for these samples decreased as annealing temperature increased (i.e., samples became less strongly ordered); for example, a sample of composition $\text{Ni}_{0.6}\text{Mg}_{1.4}\text{SiO}_4$ showed a decrease in K_D from 15.6 (not annealed) to 10.6 (sample quenched from 800 °C) to 5.7 (quenched from 1300 °C). Note that Boström (1989) reported an even lower K_D (4.76) for his sample of this composition quenched from 1300 °C. Bearing in mind the suggestion that inter-site ordering in Fe-Mg olivines takes place on a time-scale of about 10 ms or less at 1000 °C (Aikawa et al. 1985), even the results of

Ottonello et al. (1989) and Boström (1989) must be treated with caution.

Important in situ olivine ordering experiments were carried out at 800 °C and 4 GPa on a synthetic sample of composition NiMgSiO_4 by Chen et al. (1996). The K_D was found to increase to 9.39 at high P compared to the starting value at room T and P ($K_D = 8.3$) over a time period of about 40 minutes during which time it was heated from 20 to 800 °C. The sample was then held at 4 GPa and 800 °C for a further 69 minutes showing a further increase of K_D to 10.25. Chen et al. (1996) suggested that Ni-Mg diffusion between M1 and M2 is relatively slow; it is difficult, however, to separate the effects of time, P and T in this variable temperature experiment.

The fact that site ordering occurs between M1 and M2 points to the non-ideality of the Ni-Mg olivine solid solution series and this is confirmed by variation of the b unit-cell parameter as a function of composition, and the marked positive excess volumes of mixing (Matsui and Syono 1968). Despite these indications, Campbell and Roeder (1968) reported that phase equilibrium experiments at controlled oxygen fugacities were consistent with the Ni-Mg olivine series being close to ideal with small positive deviations from ideality at 1400 °C, consistent with maximum values for activity coefficients of 1.18. Subsequently, Seifert and O'Neill (1987) confirmed the presence of small positive deviations from ideal mixing at 1220 K and 0.1 MPa, and at 1573 K and 0.5 GPa, which could be described by a simple regular solution with the parameter $W_{\text{ol}}(\text{Ni-Mg}) = 0.35 \pm 1.0$ kJ/g-atom. Boström and Rosén (1988) also describe very small positive deviations for Ni-rich compositions at 1400 K, and small negative deviations across the compositional range at 1200 K. Ottonello et al. (1989) used X-ray single-crystal structural data to develop a thermodynamic model which showed near-ideal behavior over a range of temperatures from 600 to 1400 °C. Fleet (1989) determined experimentally the distribution of Ni between coexisting (Fe,Ni)S and (Mg,Fe,Ni)₂SiO₄ and, for Ni-olivine mole fractions between 0.004 and 0.014 at 1300–1395 °C and 1 bar, deduced that positive deviations from ideality occurred (maximum $\gamma = 1.75$). Hirschmann (1991, 1992) used a very comprehensive database of published work to establish a general thermodynamic model for minor element (Ni, Ca, Mn, Co) M1-M2 exchange in Mg-Fe olivines. This model is based on cation ordering and symmetrical enthalpies of mixing (cation exchange), but assumed that no excess entropies of exchange occurred ($\Delta S_{\text{ex}} = 0$; thus effectively $\Delta G_{\text{ex}} = \Delta H_{\text{ex}}$). Hirschmann deduced that solution of Ni in Mg-Fe olivines was accompanied by small negative variations from ideality for Fe-free samples which became more negative in ferromagnesian olivines; a value for $\Delta H_{\text{ex}}(\text{Ni-Mg})$ of 12.5 ± 2.5 kJ/mol was reported. Hirschmann (1992) suggested that the positive deviations from ideality reported by Fleet (1989) were unreliable and this topic has been the subject of recent debate (Fleet 2000; Hirschmann 2000) without resolution. Nikitina (1992) used a theoretical “quasichemical model for multisublattice low-symmetrical solid solutions” to deduce that (Mg,Ni)₂SiO₄ solid solutions show a positive departure from ideality with $W_{\text{ol}}(\text{Ni-Mg}) = 1.65 \pm 0.84$ kcal/mol.

None of the thermochemical studies provide data supporting either the substantial negative deviations from ideality suggested by Bish (1981) or the significant positive deviations reported by Ottonello and Morlotti (1987). Note that negative deviations from ideality are consistent with a tendency towards cation ordering, with potential compound formation, while positive deviations are indicative of clustering and potential immiscibility (Davies and Navrotsky 1981; Boström and Rosén 1988).

The utility of thermodynamic models which involve cation intersite ordering data determined at room T clearly depends on the extent to which high T cation distributions were quenched-in, following synthesis or annealing experiments. Thus structural work at high temperatures is necessary to es-

tablish reliably the T - and composition-dependence of M1-M2 ordering; Hirschmann (1992, 2000) and Snyder (1993) obtained such data using single-crystal X-ray methods. Unfortunately, the data of Hirschmann (1992) for individual samples show little systematic variation of K_D with temperature with only the sample of composition $\text{Mg}_{0.56}\text{Ni}_{1.44}\text{SiO}_4$ showing an adequate linear trend of $\ln K_D$ vs. $1/T$ (K) leading to a reliable ΔH_{ex} of 19.3 kJ/mol. However, Hirschmann (1992, 2000) used individual exchange energies for each structure determination ($\Delta G_{\text{ex}} = -RT \ln K_D$ for temperatures of 800, 900, and 1000 °C) and his thermodynamic model to obtain an estimate for ΔH_{ex} of 19.5 kJ/mol for Ni-Mg exchange. Hirschmann also concluded that ΔG_{ex} showed compositional dependence varying from ~ 22.5 kJ/mol at $\text{Mg}_{1.78}\text{Ni}_{0.22}\text{SiO}_4$ to around ~ 14 – 18 kJ/mol for $\text{Mg}_{0.28}\text{Ni}_{1.72}\text{SiO}_4$. The ΔG_{ex} values obtained by Snyder for $\text{Mg}_{0.79}\text{Ni}_{1.21}\text{SiO}_4$ from 800 to 1300 °C average about 20 kJ/mol which Hirschmann (2000) suggested was consistent with his composition dependence trend. The high T K_D data of Snyder (1993) have quite high errors but define a reasonable linear relationship between $\ln K_D$ and $1/T$ giving a ΔH_{ex} value of about 15.5 ± 3.5 kJ/mol.

Despite the existence of all of the above work, much remains to be firmly established for the Mg-Ni olivine solid solution series.

EXPERIMENTAL METHODS

Ten gram batches of samples were prepared by mixing stoichiometric amounts of dried NiO, MgO and SiO₂ (Aldrich high purity). Samples of composition $\text{Mg}_{1.6}\text{Ni}_{0.4}\text{SiO}_4$ and $\text{Mg}_{1.0}\text{Ni}_{1.0}\text{SiO}_4$ were fired overnight at 1000 °C, reground and then fired at 1350 °C for 5 days in Pt crucibles. The Mg end member was crystallized for 5 days at 1050 °C, followed by 4 days at 1400 °C and 2 days at 1500 °C. The Ni end member was crystallized for 5 days at 1050 °C, followed by 4 days at 1400 °C and was mainly olivine with some unreacted busenite and cristobalite. Samples of composition $\text{Mg}_{1.7}\text{Ni}_{0.3}\text{SiO}_4$, $\text{Mg}_{1.5}\text{Ni}_{0.5}\text{SiO}_4$, $\text{Mg}_{1.4}\text{Ni}_{0.6}\text{SiO}_4$, and $\text{Mg}_{0.4}\text{Ni}_{1.6}\text{SiO}_4$ were heated overnight at 1050 °C, reground then heated for 3 days at 1250 °C, followed by 3 days at 1430 °C. In all cases the samples were quenched by dipping the bottom of the platinum crucible in water. The products were single-phase, green powders. As-synthesized solid solutions were all analyzed using a Cameca SX-100 wavelength dispersive electron microprobe at Manchester University confirming that they are homogeneous and on composition (Table 1). Samples for the high T experiments were pressed into 7 mm diameter pellets about 5 mm high, five of which were “sealed” into quartz glass tubes with a “buffer reservoir” of hematite above the olivine samples separated by pure silica wool. The two samples used for these in situ, neutron diffraction experiments were also analyzed after the heating experiments, and did not change composition during the high T structural studies (Table 1). Room T unit-cell parameters were determined for all samples by X-ray powder diffraction using high purity silicon as internal standard (Table 1); parameters before and after the heating experiments agreed within experimental error (Table 1).

The structural study was carried out on the ISIS, pulsed neutron source at the Rutherford Appleton Laboratory, U.K.

TABLE 1. Sample compositions and unit-cell parameters for synthetic Ni-Mg olivine samples

	Ni _{1.6} Mg _{0.4} SiO ₄	Ni _{1.0} Mg _{1.0} SiO ₄		Ni _{0.6} Mg _{1.4} SiO ₄	Ni _{0.5} Mg _{1.5} SiO ₄	Ni _{0.4} Mg _{1.6} SiO ₄		Ni _{0.3} Mg _{1.7} SiO ₄
		Before*	After*			Before	After	
	Wt%							
Number of analyses	6	90	10	6	6	96	10	6
SiO ₂	30.4(1)†	34.0(6)†	34.0(4)	37.0(2)	38.1 (1)	38.8(6)	38.6(3)	40.0(3)
MgO	8.29(6)	22.4(4)	22.5(5)	34.7(3)	38.9(2)	41.4(6)	41.0(4)	45.2(3)
NiO	59.9(3)	42.6(6)	44.0(5)	28.1(4)	22.9(1)	19.5(3)	20.7(5)	15.0(3)
CaO	n.d.	0.22(1)	0.16(2)	n.d.	n.d.	0.25(2)	0.21(3)	n.d.
FeO	0.02(2)	0.02(1)	0.03(1)	0.02(1)	0.18(2)	0.04(1)	0.03(1)	0.01(.1)
Total	98.61	99.24	100.69	99.92	100.08	99.99	100.54	100.21
	Cations/ 4O							
Si	1.002	1.001	0.993	0.999	0.998	0.999	0.995	1.004
Mg	0.408	0.982	0.977	1.394	1.517	1.590	1.574	1.688
Ni	1.587	1.008	1.032	0.608	0.482	0.404	0.430	0.302
Ca	—	0.007	0.005	—	—	0.008	0.006	—
Fe	0.0003	0.0005	0.0007	0.0003	0.004	0.0008	0.0008	0.002
	Mol%							
Mg ₂ SiO ₄	20.5	49.3	48.6	69.6	75.9	79.8	78.6	84.8
Ni ₂ SiO ₄	79.5	50.7	51.4	30.4	24.1	20.2	21.4	15.2
	Unit cell							
<i>a</i> , Å	4.7310(6)	4.7396(5)	4.7376(7)	4.7460(7)	4.7473(6)	4.7487(6)	4.7490(5)	4.7515(5)
<i>b</i> , Å	10.144(1)	10.187(1)	10.186(1)	10.194(2)	10.196(2)	10.201(1)	10.201(1)	10.199(1)
<i>c</i> , Å	5.9267(7)	5.9467(7)	5.9467(8)	5.9568(9)	5.9597(8)	5.9678(7)	5.9678(6)	5.9696(7)
<i>V</i> , Å ³	280.39(4)	287.12(4)	286.97(5)	288.19(6)	288.47(6)	289.10(5)	289.12(4)	289.29(4)

Notes: Our unit-cell parameter data for the end-members are Mg₂SiO₄ *a* = 4.756 (1), *b* = 10.197(2), *c* = 5.980(1) Å, *V* = 290.07(10) Å³; Ni₂SiO₄ *a* = 4.727(1), *b* = 10.120(1), *c* = 5.911(1) Å, *V* = 284.98(7) Å³.

* Before and after high temperature neutron diffraction experiments.

† Figures in parentheses are 1 sigma standard deviations.

The principles of the time-of-flight neutron powder diffraction technique are summarized in Redfern et al. (1997) and the experimental data collection and analysis conditions are summarized in Table 2. For the high *T* experiments, the heating cycle data for each temperature were collected in four or five steps of about 30 minutes each. At first, the data for each 30 minute interval were refined separately but little significant structural difference was observed in any experiment. During the cooling cycles, data were collected in two steps of about 30 minutes. The structural results reported here are for summed data sets at each temperature. Data were refined using the Rietveld method (Rietveld 1968) employing routines from the Cambridge crystallographic software library. Data were refined to stable convergence according to the scheme given in Table 2. Results are presented in Table 3. The room *T* structural data discussed here were all obtained by running the sample in standard sample assemblies rather than in the furnace and thus have lower estimated standard deviations.

The local environments around Ni were determined by K-edge EXAFS at 8.3 keV on Station 9.2 of the Synchrotron Radiation Source, Daresbury, operating in multi-bunch mode at an energy of 2 GeV with an average current of 150 mA. Samples were finely ground under acetone, mixed with boron nitride and mounted in sample holders with Sellotape windows. Spectra were collected at room *T* in transmission mode with ion-chamber detectors, using a Si (220) double crystal monochromator detuned to 50% rejection of the incident beam in order to remove harmonic contamination. Data out to a *k* value of 16 Å⁻¹ were collected and refined.

The raw data were summed in the Daresbury program EXCALIB and background subtracted using EXBACK. The

TABLE 2. Experimental data collection and Rietveld refinement details

Instrumental	Details
Diffractometer	POLARIS (neutron time-of-flight powder diffractometer)
Flight path	12.7837 m
Detectors	38 ³ He gas tubes, 145° 2θ
Data range	3000.0–9600.00 ms
Time channel binning	<i>dt/t</i> = 5 × 10 ⁻³
Temperature	see Table 3
Refinement	Details
Space Group	<i>Pbnm</i>
<i>Z</i>	4
Unit cell refinement	whole pattern
Observations	2200–3000
Refined parameters	
Structural	20
Profile	4
Background	10 Chebyshev polynomials of the first kind
Cell	3
Constraints	
strict (equal <i>B</i> _{iso})	Mg1=Ni1, Mg2=Ni2
strict (Σsite = 1.0)	Mg1+Ni1, Mg2+Ni2 Ni1 + Ni2 = <i>x</i> (<i>x</i> = Ni atoms p.f.u.), Mg1 + Mg2 = 2 - <i>x</i>
Thermal parameters	all atoms isotropic
Agreement factors (χ ² = [<i>R</i> _{wp} / <i>R</i> _{exp}] ²)	see Table 3

isolated *k*³-weighted EXAFS data were analyzed using EXCURV98 (Binsted 1998), employing the single scattering spherical wave theory (Lee and Pendry 1975; Gurman et al. 1984). Phaseshifts were derived from ab initio calculations using Hedin-Lundqvist potentials and programme default values of the muffin tin radius and ionicity (Hedin and Lundqvist 1969). No Fourier filtering was used. For each spectrum a theo-

retical fit was obtained by adding shells of backscattering atoms around the central absorber atom and iterating the the Fermi energy correction (E_f), the absorber-scatterer distances (r) and the Debye-Waller factors ($2\sigma^2$) for all shells to get the best agreement with the experimental data; no coordination numbers were refined. The Debye-Waller factors include contributions from the thermal motion of the absorber-scatterer pairs and also a static contribution from any variation in r between the scatterers in one shell. O atoms beyond 4.0 Å were not included as scattering from these makes an insignificant contribution to the EXAFS and shells beyond 4.4 Å were not refined as this would have involved more variable parameters than the data justified. Initially only the first shell was included in the simulation and the outer shells were added sequentially. After all the shells for the model were included, the Ni:Mg occupancy of the outer M shells in the model was refined. Relative errors in the first-shell bond distance are ± 0.01 Å with probable absolute errors of ± 0.02 Å. Errors for Debye-Waller factors are about $\pm 20\%$.

RESULTS AND STRUCTURAL INTERPRETATIONS

X-ray powder diffraction room T unit-cell parameters vs. composition

The unit-cell parameters for our samples together with data from the literature for synthetic Ni-Mg olivines are shown in Figure 1; the literature values shown for the end members are average values based on data from Matsui and Syono (1968), Hazen (1976), Brown (1982), Fujino et al. (1981), Boström (1987), Della Giusta et al. (1990), and Cernik et al. (1990). Our end member data are within error of the mean literature values. For the solid solutions, the data sets of Matsui and Syono (1968), Boström (1987), and Hirschmann (1992) and our samples define trends with composition for the a and c unit-cell parameters which are essentially linear. The Matsui and Syono (1968), Boström (1987), Hirschmann (1992) and our data define a clear trend for b which shows a very marked positive departure from linearity, with either a "plateau" up to about $X_{\text{Ni}} = 0.30$, or possibly even a maximum at about $X_{\text{Ni}} = 0.20$. Note, however, that the b unit-cell parameter depends on both the bulk composition and the degree of disorder between M1 and M2, with b decreasing as disorder increases for a given bulk composition (Ottonello et al. 1989; Boström 1989). The unit-cell volume data for the Ni-Mg samples also shows clear departure from Vegard's Law with positive volumes of mixing. By contrast to these trends, the a , b , c , and V parameters for the Ni-Mg solid solution samples from Rajamani (1975), Bish (1981), Snyder (1993), and Chen et al. (1996) all plot below those for the other data, and indeed have volumes plotting on a linear trend between the end-members. It is almost certain that discrepancies between the unit-cell parameter vs. composition trends reported by different workers reflect systematic errors due to the lack of adequate d spacing standardisation. Note that, in this context, Matsui and Syono (1968) used an external Si standard and we used internal Si standardisation. We therefore place most reliance on those data sets but the data of Boström (1987) and Hirschmann (1992) are in very good agreement with the preferred data sets.

The possible maximum in the b unit-cell parameter close to $X_{\text{Ni}} = 0.20$ is very similar to that found for the b parameter in Fe-Mn olivines (Annersten et al. 1984; Ballet et al. 1987; Redfern et al. 1998) which shows a maximum in the region $X_{\text{Mn}} = 0.7-0.8$. This relationship might point to a fundamental crystal chemical discontinuity within the Mg-Ni and Mn-Fe olivine solid solution series at least, whereby the substitution of 20–30 mol% of the end-member with the smaller b parameter causes a small but significant increase in b .

Room temperature neutron powder diffraction structural data vs. composition

Room T atomic coordinates, temperature factors, Ni site occupancies for the M1 site, and octahedral site ordering parameters are given in Table 3, together with χ^2 fit data ($\chi^2 = R_{\text{wp}}^2/R_{\text{exp}}^2$). χ^2 for structural data obtained at room T without the furnace are around 6.0. Structural parameters are plotted as a function of composition in Figures 2 to 5.

Cation ordering on M1 and M2 sites. The variations of Ni occupancy of M1 and M2 with bulk composition for our Ni-Mg olivine samples are displayed in Figure 2 and show a smooth increase with increasing bulk Ni_2SiO_4 content. As expected, the Ni is distinctly ordered into the M1 site. Figure 2 shows that our samples are more disordered than those of Boström (1987) and Hirschmann (1992) with similar bulk compositions to ours, and have the same degree of order as two of Boström's (1989) "fast quenched" samples. Our samples are generally slightly more ordered than the "fast quenched" samples of Ottonello et al. (1989) and Boström's (1989) sample of composition $X_{\text{Ni}} = 0.30$. Values for the distribution coefficient $K_D [= (\text{Ni}/\text{Mg})^{\text{M1}}/(\text{Ni}/\text{Mg})^{\text{M2}}$] vs. bulk composition are shown in Figure 3a while equivalent values for an order parameter $Q = 1 - (Y/X)$ are shown in Figure 3b (Y is the Ni occupancy of M1 and X is the proportion of Ni in the mineral stoichiometry). For complete disorder over the two sites $K_D = 1.0$ and $Q = 0$, while for ordering of Ni into M1, $K_D \rightarrow \infty$ and $Q \rightarrow 1$, and for "antiordeering" of Ni into M2, $K_D \rightarrow 0$ and $Q \rightarrow -1$. The K_D values increase with decreasing Ni_2SiO_4 content reaching a maximum value of 9.5 at a composition with $X_{\text{Ni}} = 0.20$, before decreasing again to 8.4 at a value of 0.15. The Q values show a linear trend over the range $X_{\text{Ni}} = 0.2-0.8$ but then flatten off at 0.15–0.20. Note that the maximum in the K_D trend and the leveling off of the Q trend coincides with the possible maximum observed for the b unit-cell parameter values.

Octahedral cation-O distances and bond angles. The absolute M1-O and M2-O bond lengths and mean M-O distances for our samples are shown in Figure 4. The trends with composition are very similar to those for the Ni-Mg series figured by Boström (1987), as reflected in the excellent agreement between our data and his end-member values which are also included in Figure 4. The lines in Figure 4 join the end-member values and it might be expected that solid solutions with completely disordered Ni and Mg on both M1 and M2 would fall on these linear trends. As predicted by Boström (1987, 1989), ordering of smaller Ni into M1 and larger Mg into M2 should produce, respectively, negative and positive deviations from these trends. In fact, our samples generally show only small departures from these linear trends. Nevertheless, our Ni-poor

TABLE 3. Structural data at room and elevated temperatures

	<i>a</i> (Å)	<i>b</i> (Å)	<i>c</i> (Å)	Si <i>x</i>	Si <i>y</i>	Si <i>B</i> _{iso}	O1 <i>x</i>	O1 <i>y</i>	O <i>B</i> _{iso}	O2 <i>x</i>
Samples at room temperature										
Mg _{1.7} Ni _{0.3} SiO ₄	4.7515(5)	10.199(1)	5.9696(7)	0.4256(1)	0.0938(1)	0.24(1)	0.7667(1)	0.0924(1)	0.41(1)	0.2211(1)
Mg _{1.8} Ni _{0.4} SiO ₄	4.7487(6)	10.201(1)	5.9678(7)	0.4253(1)	0.0936(1)	0.28(1)	0.7664(1)	0.0924(1)	0.45(1)	0.2218(1)
Mg _{1.5} Ni _{0.5} SiO ₄	4.7473(6)	10.196(2)	5.9597(8)	0.4256(1)	0.0937(1)	0.26(1)	0.7670(1)	0.0927(1)	0.42(1)	0.2208(1)
Mg _{1.4} Ni _{0.6} SiO ₄	4.7460(7)	10.194(2)	5.9568(9)	0.4255(1)	0.0936(1)	0.25(1)	0.7675(1)	0.0928(1)	0.41(1)	0.2206(1)
Mg _{1.0} Ni _{1.0} SiO ₄	4.7396(5)	10.187(1)	5.9467(7)	0.4256(2)	0.0933(1)	0.29(1)	0.7677(1)	0.0931(1)	0.44(1)	0.2203(1)
Mg _{0.4} Ni _{1.6} SiO ₄	4.7310(6)	10.144(1)	5.9267(7)	0.4264(2)	0.0935(1)	0.25(1)	0.7701(2)	0.0936(1)	0.38(1)	0.2180(2)
Samples at elevated temperature										
T °C; Mg_{1.0}Ni_{0.0}SiO₄										
25	4.74016(4)	10.1874(1)	5.94729(5)	0.4261(4)	0.0922(3)	0.05(2)	0.7678(4)	0.0928(2)	0.26(2)	0.2209(4)
200	4.74800(3)	10.2114(1)	5.96047(3)	0.4250(4)	0.0936(2)	0.31(2)	0.7686(4)	0.0931(2)	0.54(2)	0.2210(4)
300	4.75177(3)	10.2259(1)	5.96665(4)	0.4253(4)	0.0934(2)	0.37(2)	0.7683(4)	0.0933(2)	0.64(2)	0.2210(4)
400	4.75574(3)	10.2344(1)	5.97318(4)	0.4254(4)	0.0935(2)	0.44(2)	0.7680(4)	0.0933(2)	0.74(2)	0.2214(3)
450	4.75871(3)	10.2407(1)	5.97656(4)	0.4252(4)	0.0934(2)	0.49(2)	0.7679(4)	0.0932(2)	0.79(2)	0.2213(3)
500	4.75984(4)	10.2469(1)	5.97999(4)	0.4252(4)	0.0932(2)	0.52(2)	0.7676(4)	0.0932(2)	0.85(2)	0.2213(4)
550	4.76202(3)	10.2534(1)	5.98349(4)	0.4251(4)	0.0931(3)	0.54(3)	0.7674(4)	0.0934(2)	0.88(3)	0.2212(3)
600	4.76419(3)	10.2603(1)	5.98710(4)	0.4254(4)	0.0929(2)	0.60(3)	0.7672(4)	0.0935(2)	0.94(3)	0.2215(4)
650	4.76626(3)	10.2672(1)	5.99066(4)	0.4251(4)	0.0930(2)	0.63(3)	0.7672(4)	0.0935(2)	1.00(3)	0.2215(4)
700	4.76809(3)	10.2754(1)	5.99411(4)	0.4252(4)	0.0929(2)	0.69(3)	0.7670(4)	0.0936(2)	1.08(3)	0.2216(4)
750	4.77029(4)	10.2835(1)	5.99796(1)	0.4251(4)	0.0927(2)	0.73(3)	0.7667(4)	0.0936(2)	1.14(3)	0.2218(4)
800	4.77267(4)	10.2901(1)	6.00184(5)	0.4250(4)	0.0927(2)	0.76(3)	0.7664(4)	0.0935(2)	1.21(3)	0.2214(4)
850	4.77504(4)	10.2960(1)	6.00539(5)	0.4252(4)	0.0926(2)	0.81(3)	0.7662(4)	0.0936(2)	1.26(3)	0.2215(4)
900	4.77773(4)	10.3026(1)	6.00950(5)	0.4251(5)	0.0925(3)	0.86(3)	0.7662(5)	0.0935(2)	1.36(3)	0.2217(4)
950	4.78014(4)	10.3088(1)	6.01327(6)	0.4253(4)	0.0923(2)	0.90(3)	0.7662(4)	0.0936(2)	1.40(3)	0.2216(4)
1000	4.78269(5)	10.3155(1)	6.01747(6)	0.4250(4)	0.0924(2)	0.95(3)	0.7661(4)	0.0937(2)	1.45(3)	0.2218(4)
1050	4.78522(5)	10.3224(1)	6.02158(6)	0.4253(5)	0.0926(3)	0.99(3)	0.7658(5)	0.0936(2)	1.51(3)	0.2218(4)
1100	4.78795(5)	10.3296(1)	6.02598(6)	0.4254(5)	0.0922(3)	1.03(3)	0.7660(5)	0.0939(2)	1.61(3)	0.2217(5)
850c	4.77555(6)	10.2926(1)	6.00582(6)	0.4250(4)	0.0922(2)	0.79(3)	0.7664(4)	0.0936(2)	1.26(3)	0.2219(4)
750c	4.77091(5)	10.2828(1)	5.99795(6)	0.4247(4)	0.0928(2)	0.74(3)	0.7668(4)	0.0934(2)	1.14(3)	0.2216(4)
650c	4.76655(5)	10.2694(1)	5.99104(6)	0.4254(4)	0.0931(2)	0.61(3)	0.7671(4)	0.0934(2)	0.98(3)	0.2213(4)
550c	4.76218(4)	10.2564(1)	5.98397(6)	0.4251(4)	0.0931(2)	0.55(3)	0.7674(4)	0.0933(2)	0.87(3)	0.2215(4)
350c	4.75397(4)	10.2317(1)	5.97049(5)	0.4250(4)	0.0936(2)	0.42(2)	0.7680(4)	0.0934(2)	0.69(2)	0.2212(4)
25c	4.73717(2)	10.1870(1)	5.94660(3)	0.4256(2)	0.0932(2)	0.22(1)	0.7679(2)	0.0932(1)	0.33(1)	0.2203(2)
T °C; Mg_{1.0}Ni_{0.0}SiO₄										
25	4.74955(3)	10.2019(1)	5.96718(3)	0.4258(3)	0.0939(2)	0.14(2)	0.7672(3)	0.0926(1)	0.29(2)	0.2223(3)
200	4.75769(2)	10.2279(1)	5.98117(3)	0.4257(3)	0.0938(2)	0.31(2)	0.7667(3)	0.0926(1)	0.51(2)	0.2223(3)
300	4.76127(2)	10.2391(1)	5.98720(3)	0.4254(3)	0.0937(2)	0.36(2)	0.7663(3)	0.0927(1)	0.56(2)	0.2223(3)
400	4.76517(3)	10.2566(1)	5.99363(3)	0.4256(3)	0.0935(2)	0.43(2)	0.7660(3)	0.0927(1)	0.70(2)	0.2223(3)
450	4.76710(3)	10.2573(1)	5.99691(3)	0.4256(3)	0.0932(2)	0.48(2)	0.7659(3)	0.0927(1)	0.75(2)	0.2223(3)
500	4.76919(3)	10.2639(1)	6.00034(3)	0.4257(4)	0.0932(2)	0.50(2)	0.7658(4)	0.0927(1)	0.80(2)	0.2226(3)
550	4.77133(3)	10.2707(1)	6.00390(3)	0.4255(4)	0.0931(2)	0.55(2)	0.7657(4)	0.0926(1)	0.85(2)	0.2224(3)
600	4.77346(3)	10.2781(1)	6.00745(4)	0.4256(4)	0.0931(2)	0.59(2)	0.7653(3)	0.0923(2)	0.92(2)	0.2226(3)
650	4.77567(3)	10.2856(1)	6.01107(4)	0.4254(4)	0.0928(2)	0.63(2)	0.7652(4)	0.0928(2)	0.99(2)	0.2227(3)
700	4.77799(3)	10.2928(1)	6.01488(4)	0.4252(4)	0.0929(2)	0.66(2)	0.7651(4)	0.0926(2)	1.04(2)	0.2226(4)
750	4.78036(3)	10.2998(1)	6.01881(4)	0.4253(4)	0.0928(2)	0.71(2)	0.7650(4)	0.0930(2)	1.10(3)	0.2227(4)
800	4.78256(3)	10.3064(1)	6.02259(4)	0.4255(4)	0.0927(2)	0.76(3)	0.7647(4)	0.0927(2)	1.16(3)	0.2227(4)
850	4.78467(3)	10.3127(1)	6.02620(4)	0.4256(4)	0.0926(2)	0.78(3)	0.7649(4)	0.0928(2)	1.22(3)	0.2226(4)
900	4.78701(3)	10.3194(1)	6.03014(5)	0.4257(4)	0.0925(2)	0.83(3)	0.7644(4)	0.0928(2)	1.30(3)	0.2228(4)
950	4.78910(4)	10.3259(1)	6.03362(5)	0.4257(4)	0.0925(2)	0.89(3)	0.7641(4)	0.0928(2)	1.37(3)	0.2228(4)
1000	4.79136(4)	10.3323(1)	6.03741(6)	0.4253(4)	0.0927(3)	0.93(3)	0.7641(4)	0.0931(2)	1.44(3)	0.2229(4)
1100	4.79608(6)	10.3467(1)	6.04574(7)	0.4257(5)	0.0926(3)	1.01(4)	0.7639(5)	0.0929(2)	1.58(4)	0.2231(5)
300c	4.75898(4)	10.2340(1)	5.98423(5)	0.4259(3)	0.0937(2)	0.37(2)	0.7664(3)	0.0926(2)	0.60(2)	0.2222(3)
25c	4.74737(2)	10.2069(1)	5.96790(3)	0.4256(2)	0.0937(1)	0.21(1)	0.7666(2)	0.0926(2)	0.35(1)	0.2219(2)

Notes: Data labeled c are cooling runs; numbers in brackets are 1 σ standard deviations.

solid solutions do seem to show significant positive departures for M2-O2 and negative departures for M1-O2; the M1-O1, M2-O1, M2-O3a and mean M2-O distances for the sample with $X_{Ni} = 0.20$ also plot slightly above the linear join. Note that the cumulative effects of individual M-O displacements from the linear join between the end members cancel out for the M1 octahedron, but are additive for M2. Boström (1987) did not observe anomalously long M-O distances for any of his samples, presumably because the solid solution with the lowest Ni content was too Ni-rich at $X_{Ni} = 0.30$. The possible maximum in *b* at $X_{Ni} = 0.20$ coincides with anomalous lengthening at M1-O1 and shortening at M1-O2, equivalent to a shear of the quadrilateral formed by O1 and O2 atoms at the M1 site. Thus the

distortion at the M1 site is a maximum at this composition, while the main effect at M2 is on the octahedral volume. Coupling between these effects is mediated through the shared edges of the octahedra and tetrahedra.

The individual O-M-O bond angles (not illustrated) show smooth variations with composition with no samples plotting significantly away from the overall trends. The octahedral angle variance (Robinson et al. 1971) trends for our solid solutions are shown in Figure 4c together with end-member data from Boström (1987), and the fast-quenched annealed samples of Boström (1989) and Ottonello et al. (1989). The O-M1-O angular variance for all of the samples displayed are somewhat scattered around the join between the end members, with the

TABLE 3. continued

O2 y	O B ₈₀	O3 x	O3 y	O3 z	O B ₈₀	Ni in M1	Ni B ₈₀	M2 x	M2 y	M B ₈₀	K ₀	chi ²
Samples at room temperature												
0.4468(1)	0.43(1)	0.2766(1)	0.1629(1)	0.0328(1)	0.44(1)	0.260(2)	0.37(1)	0.9909(1)	0.2769(1)	0.45(1)	8.43	6.44
0.4467(1)	0.47(1)	0.2765(1)	0.1626(1)	0.0324(1)	0.49(1)	0.348(2)	0.39(1)	0.9910(1)	0.2768(1)	0.48(1)	9.73	5.89
0.4464(1)	0.45(1)	0.2763(1)	0.1627(1)	0.0325(1)	0.45(1)	0.424(2)	0.39(1)	0.9908(1)	0.2765(1)	0.45(1)	8.95	5.63
0.4463(1)	0.44(1)	0.2760(1)	0.1627(1)	0.0324(1)	0.43(1)	0.495(2)	0.39(1)	0.9908(1)	0.2763(1)	0.44(1)	8.36	6.07
0.4458(1)	0.47(1)	0.2756(1)	0.1624(1)	0.0316(1)	0.48(1)	0.727(3)	0.40(1)	0.9914(2)	0.2754(1)	0.44(1)	7.10	5.60
0.4452(1)	0.45(1)	0.2747(1)	0.1627(1)	0.0305(1)	0.40(1)	0.932(3)	0.40(1)	0.9927(2)	0.2744(1)	0.40(1)	6.81	8.35
Samples at elevated temperature												
T °C; Mg_{1-x}Ni_xSiO₄												
0.4460(2)	0.28(2)	0.2751(3)	0.1625(1)	0.0329(2)	0.24(2)	0.727(8)	0.22(2)	0.9919(5)	0.2758(2)	0.23(2)	7.10	8.20
0.4458(2)	0.52(2)	0.2753(2)	0.1621(1)	0.0319(2)	0.52(2)	0.729(7)	0.50(2)	0.9922(4)	0.2760(1)	0.49(2)	7.26	11.10
0.4460(2)	0.61(2)	0.2755(3)	0.1622(1)	0.0322(2)	0.62(2)	0.731(7)	0.60(2)	0.9918(4)	0.2761(1)	0.60(2)	7.38	9.22
0.4464(2)	0.71(2)	0.2756(2)	0.1621(1)	0.0323(2)	0.74(2)	0.732(6)	0.71(2)	0.9918(4)	0.2763(1)	0.70(2)	7.45	7.55
0.4463(2)	0.75(2)	0.2757(2)	0.1619(1)	0.0323(2)	0.78(2)	0.732(6)	0.76(2)	0.9916(4)	0.2765(1)	0.75(3)	7.48	7.01
0.4465(2)	0.81(3)	0.2758(2)	0.1619(1)	0.0324(2)	0.82(2)	0.726(3)	0.80(2)	0.9912(4)	0.2765(1)	0.84(3)	7.00	7.07
0.4467(2)	0.86(3)	0.2758(3)	0.1619(1)	0.0327(2)	0.89(2)	0.731(7)	0.86(2)	0.9912(5)	0.2766(2)	0.89(3)	7.35	8.55
0.4467(2)	0.92(3)	0.2759(2)	0.1619(1)	0.0326(2)	0.94(2)	0.730(7)	0.91(2)	0.9911(5)	0.2767(1)	0.95(3)	7.30	6.37
0.4469(2)	0.98(3)	0.2759(3)	0.1619(1)	0.0327(2)	1.00(2)	0.740(7)	0.97(2)	0.9907(5)	0.2768(2)	1.01(3)	8.09	6.34
0.4469(2)	1.02(2)	0.2759(3)	0.1618(1)	0.0328(2)	1.05(2)	0.746(7)	1.02(2)	0.9903(5)	0.2768(2)	1.09(3)	8.58	5.83
0.4472(2)	1.11(3)	0.2759(2)	0.1616(1)	0.0329(2)	1.11(3)	0.761(7)	1.09(2)	0.9899(5)	0.2771(2)	1.16(3)	10.13	4.06
0.4473(2)	1.16(3)	0.2761(3)	0.1617(1)	0.0330(2)	1.17(2)	0.750(7)	1.14(2)	0.9900(5)	0.2771(2)	1.22(3)	9.00	3.94
0.4475(2)	1.22(3)	0.2762(3)	0.1617(1)	0.0333(2)	1.21(2)	0.749(7)	1.21(2)	0.9895(5)	0.2774(2)	1.26(4)	8.87	4.20
0.4477(2)	1.26(3)	0.2763(3)	0.1616(1)	0.0334(2)	1.27(3)	0.732(8)	1.26(2)	0.9894(5)	0.2773(2)	1.38(4)	7.46	4.74
0.4478(2)	1.36(3)	0.2762(3)	0.1615(2)	0.0332(3)	1.34(2)	0.726(7)	1.35(2)	0.9892(5)	0.2773(2)	1.40(4)	7.01	3.76
0.4481(2)	1.39(3)	0.2765(3)	0.1617(2)	0.0335(3)	1.38(2)	0.720(7)	1.39(2)	0.9898(5)	0.2776(2)	1.49(4)	6.60	3.50
0.4481(2)	1.45(3)	0.2765(3)	0.1616(2)	0.0336(2)	1.47(3)	0.711(7)	1.47(3)	0.9897(5)	0.2777(2)	1.57(4)	6.06	3.70
0.4484(2)	1.55(3)	0.2765(3)	0.1616(2)	0.0337(3)	1.52(3)	0.702(8)	1.53(3)	0.9890(6)	0.2776(2)	1.69(4)	5.57	3.91
0.4476(2)	1.22(3)	0.2765(3)	0.1618(2)	0.0331(3)	1.24(2)	0.738(7)	1.21(2)	0.9903(5)	0.2772(2)	1.29(4)	7.95	2.77
0.4471(2)	1.08(3)	0.2762(3)	0.1618(1)	0.0330(2)	1.10(2)	0.737(7)	1.06(2)	0.9903(5)	0.2771(2)	1.19(3)	7.81	2.92
0.4468(2)	1.00(3)	0.2757(3)	0.1619(1)	0.0329(2)	1.01(2)	0.746(7)	0.96(2)	0.9905(5)	0.2769(2)	1.02(3)	8.64	3.16
0.4465(2)	0.88(3)	0.2758(3)	0.1619(1)	0.0328(2)	0.90(2)	0.743(7)	0.83(2)	0.9910(5)	0.2769(1)	0.90(3)	8.33	3.80
0.4461(2)	0.66(2)	0.2754(2)	0.1620(1)	0.0323(2)	0.67(2)	0.750(7)	0.64(2)	0.9914(4)	0.2763(1)	0.66(3)	9.04	5.03
0.4457(1)	0.36(1)	0.2756(1)	0.1625(1)	0.0318(1)	0.36(1)	0.748(4)	0.31(1)	0.9910(2)	0.2754(1)	0.30(1)	8.77	6.26
T °C; Mg_{1-x}Ni_xSiO₄												
0.4466(1)	0.31(2)	0.2757(2)	0.1627(1)	0.0324(1)	0.30(1)	0.347(6)	0.23(1)	0.9914(4)	0.2769(1)	0.29(2)	9.38	8.37
0.4471(1)	0.53(2)	0.2762(2)	0.1625(1)	0.0328(2)	0.54(1)	0.349(6)	0.48(2)	0.9911(4)	0.2773(1)	0.54(2)	9.98	10.98
0.4474(1)	0.62(2)	0.2764(2)	0.1625(1)	0.0331(2)	0.64(1)	0.351(6)	0.58(2)	0.9909(4)	0.2775(1)	0.64(2)	10.55	9.66
0.4476(1)	0.71(2)	0.2765(2)	0.1624(1)	0.0332(2)	0.74(2)	0.350(6)	0.67(2)	0.9903(4)	0.2776(1)	0.75(3)	10.15	9.35
0.4478(1)	0.76(2)	0.2766(2)	0.1624(1)	0.0333(1)	0.78(2)	0.349(6)	0.73(2)	0.9904(4)	0.2778(1)	0.81(3)	10.00	8.57
0.4479(1)	0.82(2)	0.2769(2)	0.1625(1)	0.0334(2)	0.85(2)	0.351(6)	0.79(2)	0.9902(5)	0.2778(2)	0.85(3)	10.58	9.45
0.4481(1)	0.85(2)	0.2768(2)	0.1624(1)	0.0336(2)	0.90(2)	0.352(6)	0.84(2)	0.9901(4)	0.2780(2)	0.92(3)	10.63	8.45
0.4482(1)	0.92(2)	0.2769(2)	0.1623(1)	0.0336(2)	0.95(2)	0.357(6)	0.90(2)	0.9900(5)	0.2782(2)	0.99(3)	12.50	8.14
0.4483(1)	0.98(2)	0.2770(2)	0.1624(1)	0.0337(2)	1.01(2)	0.358(6)	0.96(2)	0.9895(5)	0.2782(2)	1.06(3)	12.61	7.76
0.4485(2)	1.04(3)	0.2770(2)	0.1623(1)	0.0338(2)	1.05(2)	0.358(6)	1.00(2)	0.9894(5)	0.2784(2)	1.12(3)	12.83	8.11
0.4486(2)	1.10(3)	0.2771(2)	0.1623(1)	0.0340(2)	1.12(2)	0.358(6)	1.07(2)	0.9893(5)	0.2785(2)	1.18(3)	12.57	6.31
0.4488(2)	1.15(3)	0.2772(3)	0.1623(1)	0.0341(2)	1.18(2)	0.351(7)	1.13(3)	0.9892(5)	0.2786(2)	1.25(4)	10.44	6.62
0.4492(2)	1.12(3)	0.2772(3)	0.1623(1)	0.0341(2)	1.23(2)	0.345(7)	1.20(3)	0.9892(5)	0.2786(2)	1.36(4)	8.96	6.52
0.4494(2)	1.30(3)	0.2773(3)	0.1621(2)	0.0341(2)	1.31(2)	0.336(7)	1.27(3)	0.9891(5)	0.2789(2)	1.44(4)	7.34	6.03
0.4495(2)	1.34(3)	0.2775(3)	0.1624(1)	0.0344(2)	1.38(2)	0.337(7)	1.34(3)	0.9896(5)	0.2789(2)	1.51(4)	7.48	5.81
0.4495(2)	1.44(3)	0.2776(3)	0.1624(1)	0.0345(2)	1.43(3)	0.335(7)	1.41(3)	0.9889(6)	0.2790(2)	1.57(5)	7.25	4.41
0.4450(2)	1.54(4)	0.2778(3)	0.1622(2)	0.0347(3)	1.59(3)	0.324(8)	1.58(4)	0.9891(6)	0.2791(2)	1.72(5)	5.78	3.14
0.4474(1)	0.60(2)	0.2763(2)	0.1625(1)	0.0332(2)	0.64(1)	0.349(6)	0.58(2)	0.9910(4)	0.2775(2)	0.63(2)	9.88	9.22
0.4467(1)	0.38(1)	0.2765(1)	0.1627(1)	0.0324(1)	0.37(1)	0.349(3)	0.32(1)	0.9908(2)	0.2767(1)	0.34(1)	9.33	6.57

most disordered samples showing the largest displacement below the line. For the O-M2-O octahedral variance, most samples show a positive departure from the line. The octahedral variance trends confirm that the M2 octahedron is less distorted than M1, and that the degree of distortion decreases with increasing Ni for both sites, but with the M2 site showing the greater decrease (cf. Boström 1987). Overall, the M2-O octahedron shows the clearest departures from the linear join between the end members for both M-O distances and O-M-O angles. Lumpkin and Ribbe (1983) showed that the *b* unit-cell parameter is most strongly dependent on the size of the M2 site and thus the possible maximum in *b* observed for the sample with $X_{Ni} = 0.20$ can be correlated with its anomalously high

individual and mean M2-O bond lengths, and the anomalously high O-M2-O angular variance.

Neutron powder diffraction structural data at elevated temperatures

Unit-cell parameters, atomic coordinates, temperature factors, Ni site occupancies for the M1 site, and octahedral site ordering parameters are given in Table 3, together with χ^2 fits. χ^2 for structural data determined in the furnace range from 11.0 to 3.0, decreasing as *T* increases.

Cation ordering on M1 and M2 sites. The variations of Ni occupancy of M1 with *T* for our two samples are displayed in Figures 5a and b. When the full dataset for a given *T* are

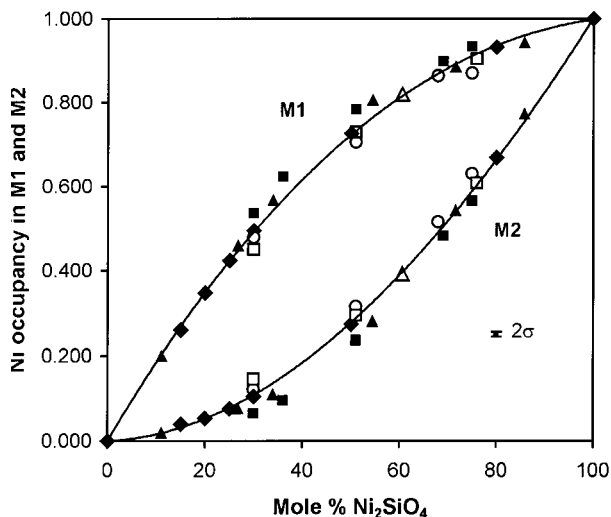


FIGURE 2. Occupancy of Ni in M1 and M2 sites vs. composition for our samples at room T (\blacklozenge) compared with those from: Böstrom (1987) \blacksquare ; Böstrom (1989) \square ; Ottonello et al. (1989) \circ ; Hirschmann (1992) \blacktriangle . A typical standard deviation for our data (2σ) is shown in the lower rhs.

refined together for each sample, significant increases in the Ni occupancy of Ni in M1 relative to that in the starting samples become apparent at 600–700 °C implying that cation ordering has changed within the timescale of our experiments (about 2.5 hours for $X_{\text{Ni}} = 0.50$ and 2 hours for $X_{\text{Ni}} = 0.20$). During the heating cycle, data were binned in 30 minute steps and refinement of successive 30 minute data sets taken at 650–700 °C for each sample show some tendency for the Ni occupancy of M1 to increase in successive 30 minute data sets, but the increments are within error. Thus at around 650 to 700 °C, the timescale of the ordering might be around 0.5 to 1 hour. Above 700 °C, each 30 minute dataset for a particular T gives essentially the same degree of order, suggesting that ordering changes might have gone to completion in less than 30 minutes for both samples.

We will discuss the order/disorder trends in terms of K_D at this stage. For sample NiMgSiO_4 at room T before the heating experiments $K_D = 7.1$. As T is increased, K_D shows no significant variation (average value of about 7.3) up to about 600 °C, above which it increases to a maximum of 10.1 at 750 °C (Fig. 5a); thus the initial trend is towards increased order in M1 (i.e., decreasing configuration entropy) as T increases. Above 750 °C the K_D decreases with increasing T , the expected trend of increasing disorder and increasing entropy. At the maximum T of our experiments (1100 °C) the K_D has decreased to 5.6. Following our earlier work on ordering in olivines (Henderson et al. 1996; Redfern et al. 1997) the initial trend towards increased ordering is attributed to kinetic effects, while the subsequent trend of increasing disorder is assumed to represent the equilibrium order/disorder trend. On cooling to around 850 °C, the ordering is reversed along the equilibrium trend but below this T the sample leaves this trend and the degree of disorder shows no significant variation. In effect, the sample has reached its “blocking temperature” for the conditions of the experiments.

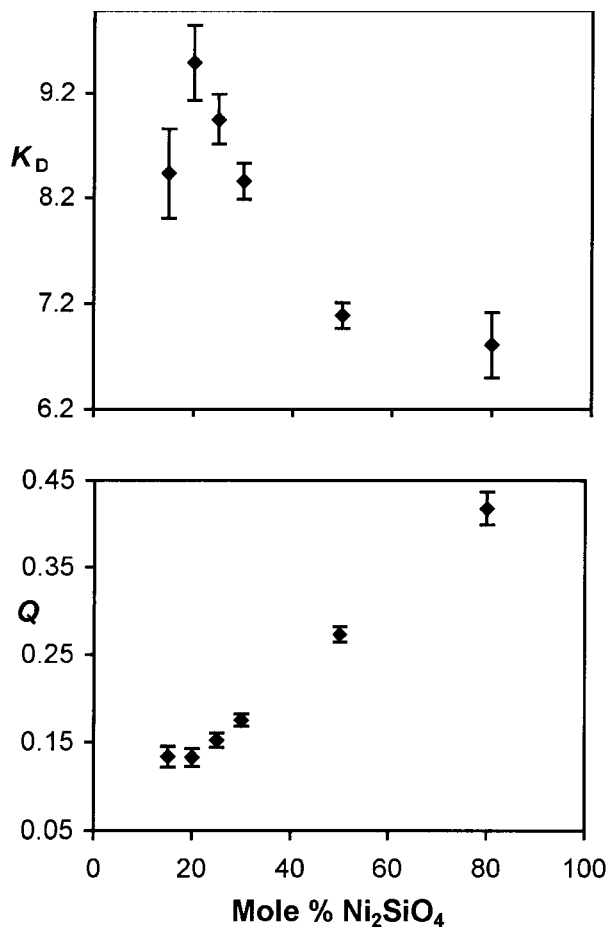


FIGURE 3. Trends for K_D (Fig. 3a) and Q (Fig. 3b) vs. bulk composition at room T . The maximum for K_D and flattening in the Q trend occur close to $\text{Mg}_{1.6}\text{Ni}_{0.4}\text{SiO}_4$, the composition associated with the possible maximum in the b unit-cell parameter trend shown in Figure 1. Standard deviations (1σ) are shown.

Note that the sample at room T before the experiments was significantly more disordered ($K_D = 7.1$) than after the heating experiments ($K_D = 8.3$) and this reflects the faster cooling from the initial synthesis temperature (cf. Redfern et al. 1996).

For sample $\text{Mg}_{1.6}\text{Ni}_{0.4}\text{SiO}_4$ the K_D before heating was 9.4 indicating that this sample is more ordered than MgNiSiO_4 . No significant change in K_D (average of about 10.1) occurs until 600 °C at which stage the sample shows a trend towards increased ordering of Ni into M1 with a maximum of 12.8 around 700 °C (Fig. 5b). Note that, although this maximum K_D value is larger than that reported for MgNiSiO_4 , the T range over which these changes occur is essentially the same for the two samples. Above 700 °C, the K_D decreases with increasing T to a value of 5.8 at 1100 °C. As found for the other sample, this curve defines the equilibrium curve for disordering in $\text{Mg}_{1.6}\text{Ni}_{0.4}\text{SiO}_4$. During cooling no structural data were collected above 300 °C. The K_D value obtained at this temperature and at room T after the experiments gave values of 10.6 and 9.9, respectively, which are slightly higher than those observed at the beginning of these experiments. These values are equivalent to

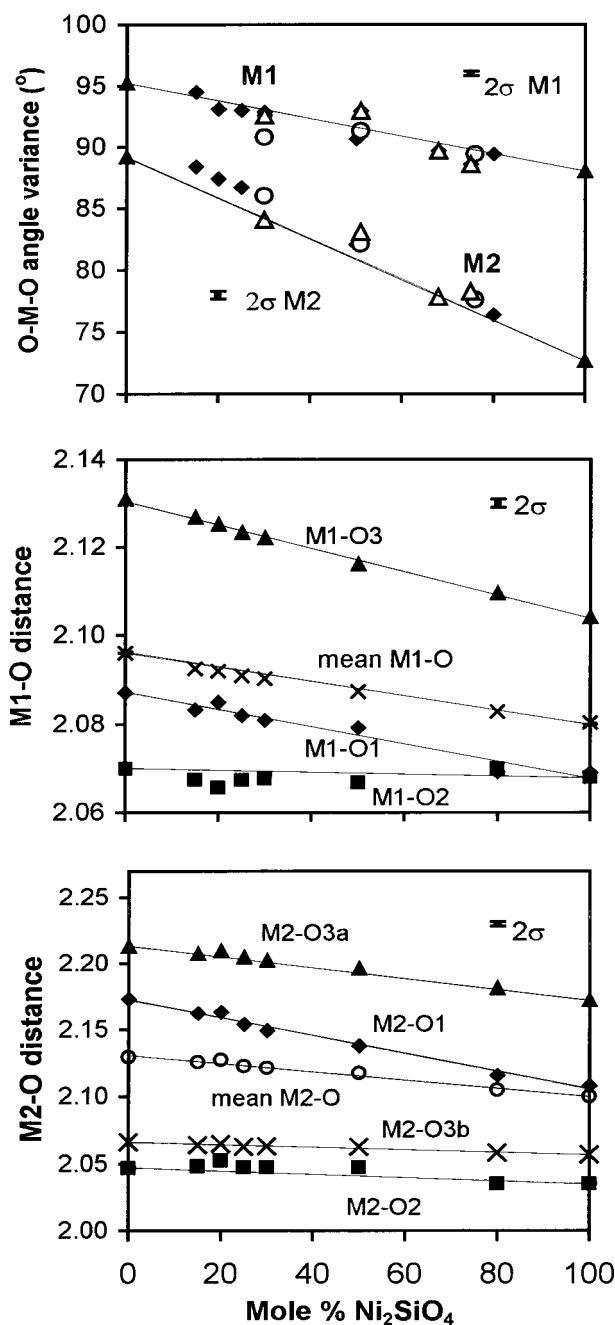


FIGURE 4. (a and b) Variation of individual and mean M-O bondlengths for the M1 and M2 octahedral sites as a function of bulk composition at room T . Data for the Mg- and Ni-end-members are from Boström (1987). Note that individual and mean M1-O and M2-O distances for $\text{Mg}_{1.6}\text{Ni}_{0.4}\text{SiO}_4$ sometimes deviate slightly but significantly from the smooth trends defined by the other samples. (c) Octahedral variance for M1 and M2 octahedral sites. The M2 site is less distorted than M1 at all temperatures and shows a greater decrease in distortion as T increases; note that the variance for M1 plots on a line between the end members while that for M2 shows a clear positive departure from linearity. Standard deviations (2σ) for our data are shown in the upper rhs of the figures. Lines join the end-member data.

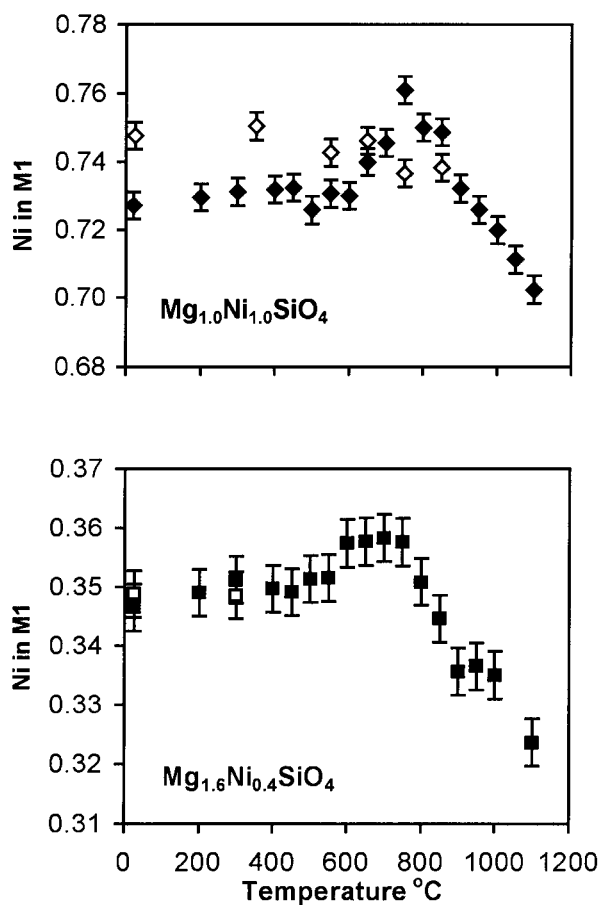


FIGURE 5. Variation of Ni occupancy of M1 for samples of composition $\text{Mg}_{1.6}\text{Ni}_{0.4}\text{SiO}_4$ and $\text{Mg}_{1.0}\text{Ni}_{1.0}\text{SiO}_4$ with increasing T . Error bars are average values and are 1σ . Solid symbols are for heating runs and open symbols are for cooling data.

about 800 °C on the equilibrium order/disorder curve suggesting a blocking T of around 800 °C for this olivine, not significantly different to that observed for MgNiSiO_4 . Although blocking temperatures depend on cooling rate, the estimate for Ni-Mg olivines are higher than that deduced for Fe-Mn olivine (Henderson et al. 1996) which suggests that the kinetics for Ni-Mg exchange might be more sluggish than those for Fe-Mn.

Despite the fact that our two samples show distinctly different degrees of order at low- T , their K_D values for each T step above 800 °C are essentially the same consistent with the equilibrium order/disorder curves being indistinguishable for our two samples. Thus, it appears that as far as equilibrium data are concerned there is no compositional dependence, at least for samples with X_{Ni} up to 0.5 and this contrasts with the data of Hirschmann (1992). The differences noted for the two samples are only obvious at temperatures below about 700–750 °C suggesting either that non-equilibrium behavior might indeed show some compositional dependence, or that the two samples experienced different cooling regimes from the synthesis temperature. We are inclined to believe the latter hypothesis as the equilibrium data do not exhibit any compositional

dependence.

Unit-cell parameters and octahedral cation-O bond lengths and angles. The absolute rates of expansion are identical for our two Ni-Mg olivine samples for each unit-cell parameter with mean expansion coefficients over the T range 25–1100 °C of $\alpha_a 0.93 \times 10^{-5} \text{ } ^\circ\text{C}^{-1}$, $\alpha_b 1.31 \times 10^{-5} \text{ } ^\circ\text{C}^{-1}$, $\alpha_c 1.23 \times 10^{-5} \text{ } ^\circ\text{C}^{-1}$ and $\alpha_v 3.52 \times 10^{-5} \text{ } ^\circ\text{C}^{-1}$. Up to 1000 °C, the relative volume expansion is identical to those for the FeMnSiO₄ and MgMnSiO₄ olivines (Redfern et al. 1997).

Both Mg_{1.6}Ni_{0.4}SiO₄ and MgNiSiO₄ show the same unit-cell-parameter relative-expansion characteristics with the expansion coefficient (α) decreasing in the order $\alpha_b > \alpha_c > \alpha_a$ (in the *Pbnm* setting). This order is the same as that found for Ni-Mg olivines with $X_{\text{Ni}} < 0.54$ (Vokurka and Rieder 1987; Hirschmann 1992), and for Mg-Mn olivine (Redfern et al. 1997). By contrast, Ni-Mg olivines with $X_{\text{Ni}} > 0.54$ (Vokurka and Rieder 1987; Hirschmann 1992; Snyder 1993) and Fe-Mn olivine (Redfern et al. 1997), show $\alpha_c > \alpha_b > \alpha_a$.

Despite the substantial discontinuities in the octahedral site ordering trends for the two samples around 600–750 °C the unit-cell parameters do not show clear changes of slope in this region. This contrasts with the trends found for FeMnSiO₄ and MgMnSiO₄ olivines (Redfern et al. 1997) which show distinct changes of slope for both *a* and *b*. Thus, the Ni-Mg site occupancies have much less effect on the overall olivine cell geometry than those for Mg-Mn, in particular, and Fe-Mn, where the size differences are greater.

With increasing T , the variations of the relative cation bond lengths (i.e., normalized relative to the room T value) for M1 and M2 polyhedra are similar for both samples (Figure 6a and b). All of the M - O bond lengths show smooth, near linear trends as T increases, with no obvious discontinuities. For M1 the thermal expansion rate decreases in the order M1-O1 > M1-O3 > M1-O2 while for M2 rates have relative values M2-O3a \approx M2-O1 \approx M2-O2 \gg M2-O3b. These values are somewhat different to those reported for the solid solutions series at room T (Boström 1987), where substitution of larger Mg for smaller Ni is accompanied by expansion of the individual bond lengths in the order: M1-O3 > M1-O1 > M1-O2, and M2-O1 > M2-O3a > M2-O3b = M2-O2. Compared to the changes accompanying substitution of Mg for Ni, the M1-O1 and M2-O2 distances show particularly high thermal expansion rates; the combination of relatively high M2-O2 and M2-O1 expansion can be correlated with the *b* axis showing the highest axial thermal expansion in our samples.

The near linear M-O trends vs. T in our samples are in clear contrast to the trends observed for the Fe-Mn and Mg-Mn olivines where obvious changes of slope are associated with the octahedral site order/disorder discontinuities near 500 °C. The mean M2-O distance expands more than that for M1-O with essentially the same expansion coefficients for both samples with values as follows: $X_{\text{Ni}} = 0.20$, M1-O 1.12×10^{-5} , M2-O 1.63×10^{-5} ; $X_{\text{Ni}} = 0.50$, M1-O 1.25×10^{-5} , M2-O $1.61 \times 10^{-5} \text{ } ^\circ\text{C}^{-1}$. These values do not represent definitive thermal expansion coefficients because of the M-O size change due to the effect of decreasing Ni in M1 and increasing Ni in M2 during disordering as T is increased along the equilibrium ordering curve from about 750 to 1100 °C. This cation size effect can be

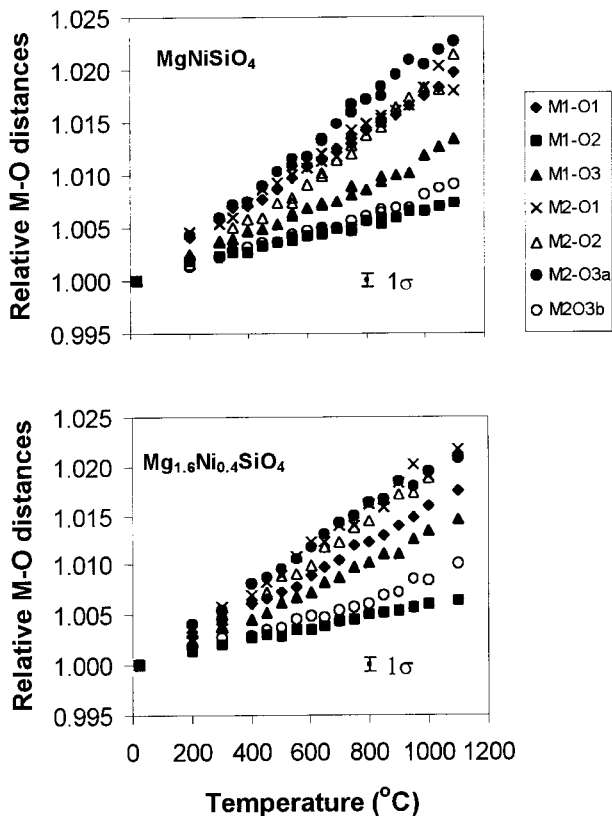


FIGURE 6. Relative expansion of individual M1-O and M2-O distances (normalized to values at room T) vs. temperature. Standard deviations (1σ) are shown.

corrected for using the room T data, giving the more reliable thermal expansion coefficients (α): $X_{\text{Ni}} = 0.20$, M1-O 1.04×10^{-5} , M2-O 1.95×10^{-5} ; $X_{\text{Ni}} = 0.50$, M1-O 1.19×10^{-5} , M2-O $1.87 \times 10^{-5} \text{ } ^\circ\text{C}^{-1}$.

For both Ni-Mg samples, the difference between the mean bond lengths for the M1-O and M2-O polyhedra [$\langle \text{M2-O} \rangle - \langle \text{M1-O} \rangle$] increases as the order parameter Q decreases. Apparently the sizes of the M1-O and M2-O polyhedra diverge as disorder increases. This contrasts with the trends found for MgMnSiO₄ and FeMnSiO₄ olivines which show decreasing ($\langle \text{M2-O} \rangle - \langle \text{M1-O} \rangle$) with decreasing Q , tending towards zero at $Q = 0$ (Redfern et al. 1997) as the two sites become much closer in size. This reflects the different driving forces for ordering in the Ni-olivines compared with the Mn-olivines, the former being dominated by crystal field effects while the latter depend on cation size differences. This effect is further illustrated in the M-site angular distortions as monitored by O-M-O angular variance data (Robinson et al. 1971). These appear to be slightly more sensitive to the effects of Ni-Mg order/disorder than bond lengths. Thus, for both samples, the variance for the M1 site shows a small but distinct increase in slope at about 750–800 °C while that for the M2 site shows a rather more subtle decrease in slope at the same T (Fig. 7). The angular variances are greater for the M1-O polyhedra than those for the M2-O polyhedra with the site distortions being larger for Mg_{1.6}Ni_{0.4}SiO₄ than for MgNiSiO₄. Both Mg-Ni samples have

significantly less distorted M-polyhedra than those found for the FeMnSiO_4 and MgMnSiO_4 samples (Redfern et al. 1997). Despite the different absolute angular variance values for the two samples, the relative changes with T are almost identical.

In summary, the behavior of the Mg-Ni olivines on disordering shows significant differences to those found for the Mg-Mn and Fe-Mn samples. It seems likely that the behavior of the Ni-Mg olivines is controlled ultimately by the strong affinity of Ni for the M1 site, resulting from its stabilization in this site by crystal-field (Wood 1974) or electronegativity (Bish 1981; Tsukimura and Sasaki 2000) effects. By contrast, the topological changes accompanying the ordering of Fe and Mn, as well as of Mg and Mn, over M1 and M2 are likely to be dominated by ionic size effects.

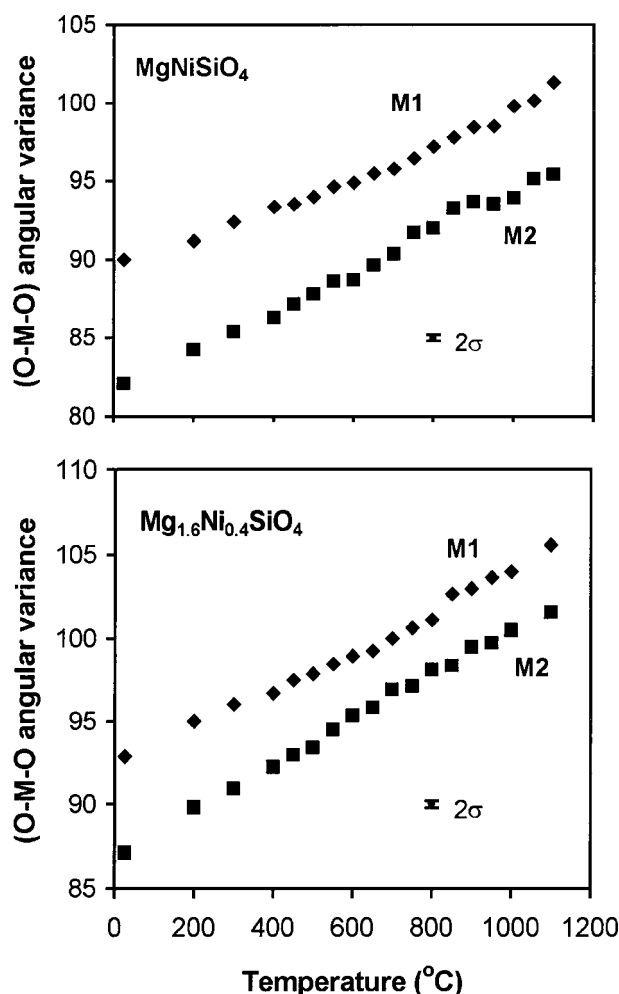


FIGURE 7. Variation in octahedral angular variance (O-M-O) as a function of T . At all temperatures the M1 site is more distorted than M2 and the degree of distortion increases with increasing T . Subtle increases in slope for M1 and decreases in slope for M2 occur near 750–800 °C, the temperature region above which M1-M2 intersite disordering is well established. Standard deviations (2σ) for our data are shown in the lower rhs.

EXAFS studies of local ordering of Ni in Ni-Mg olivines

Suggestions have been made that negative deviations from ideality in the Ni-Mg olivine solid solution series would accompany octahedral cation ordering (Bish 1981; Boström and Rosén 1988) while positive deviations for the Mg-rich end of the solid solution series could be related to either compound formation, unmixing, or cation clustering (Ottonello and Morlotti 1987; Boström and Rosén 1988). There is no evidence of two-phase behavior or sample heterogeneity on the length-scale probed by neutron and X-ray diffraction (>100 Å) and we have therefore used the element specific EXAFS technique to investigate the local environment around Ni on a length scale of <10 Å to assess whether any local clustering can be detected by refinement of the outer shell structure. In particular, the X-ray scattering contrast between Mg and Ni allows the Ni:Mg ratio in the nearest neighbor M shells to be assessed. While the EXAFS technique provides data which will be an average of the Ni environments around Ni in both the M1 and M2 sites, the crucial samples are the Mg-rich solid solutions for which a large proportion of the Ni is in the M1 site.

Green NiO (bunsenite) was run as a model compound and gave a first shell Ni-O bond length of 2.08 Å and a Debye-Waller factor of 0.015 Å² with the coordination number (CN) fixed at 6.0; the first shell bond length shows excellent agreement with the X-ray diffraction value of 2.089 Å, confirming that the ab initio fitting parameters are reliable. The 1s-3d pre-edge height for NiO is 0.025 compared to the height of the absorption edge step, a value typical of divalent Ni in six-coordinated sites. The olivine samples all have pre-edge heights of 0.02–0.025 typical of divalent Ni in octahedral sites, and the XANES spectra (not illustrated) are very similar except that a very weak feature in the Mg-rich bulk compositions is weaker still in the MgNiSiO_4 sample and essentially absent in the sample with $X_{\text{Ni}} = 0.80$, presumably linked to the increasing proportion of total Ni in M2 in these two samples.

The EXAFS model used in the Ni-Mg olivine refinements is based on single crystal X-ray data for synthetic MgNiSiO_4 (Ottonello et al. 1989) and is summarized in Table 4. The room T neutron diffraction results were used to define the overall proportions of Ni in M1 and M2 sites. This in turn fixes the average number of scatterers for each shell in the EXAFS fit. The initial proportions of Ni:Mg in M1 and M2 were chosen assuming complete homogeneity and all the distances and Debye-Waller factors were refined to obtain the initial fit for a model consisting of the first 9 shells listed in Table 4 (note that coordination numbers were not refined). The Ni-O first shell bondlengths and Debye-Waller factors showed no significant variation between samples with mean values of 2.08 ± 0.01 Å and 0.015 ± 0.003 Å², respectively. The bond length is identical to the single crystal value determined for Ni-O in the M1 site of Ni_2SiO_4 olivine (Boström 1987) and to the Ni-O bond length reported for minor element Ni (0.44 wt% NiO) in San Carlos olivine (Galoisy et al. 1995), confirming that M1 is the main site for Ni in olivine.

The fit parameters (R) for this first stage in the refinements of our samples are listed in column 2 of Table 5. The ratio of Ni:Mg in site M1 was then refined for each sample, together

TABLE 4. Radial distribution of atoms around M1 and M2 sites in synthetic MgNiSiO₄ olivine

Shell	Site M1		Site M2	
	Scatterer	<i>r</i> , Å	Scatterer	<i>r</i> , Å
1	6 × O	2.087	6 × O	2.118
2	2 × Si	2.683	1 × Si	2.769
3	2 × M1	2.972	—	—
4	2 × M2	3.171	2 × M1	3.171
5	2 × Si	3.242	4 × Si	3.266
6	2 × O	3.490	3 × O	3.495
7	4 × M2	3.614	4 × M1	3.614
8	8 × O	3.743	3 × O	3.743
9	—	—	4 × M2	3.836
10	2 × O	4.039	10 × O	3.946–4.433
11	2 × Si	4.409	—	—
12	10 × O	4.547–4.714	2 × O	4.736
13	2 × M1	4.740	2 × M2	4.740
14	2 × Si	4.986	2 × Si	5.180
15	2 × M2	5.265	2 × M1	5.265
16	2 × Si	5.308	5 × Si	5.496
17	—	—	2 × M2	5.457
18	4 × M2	5.543	4 × M1	5.543
19	8 × M1	5.604	4 × M2	5.614
20	4 × M2	5.703	4 × M1	5.703
21	2 × M1	5.944	2 × M2	5.944

with the distances and Debye-Waller factors, starting first from a low Ni percentage and then starting with a high Ni percentage. For each sample, the mean *R* values and means of the two M1 Ni site occupancy estimates are reported in Table 5 (columns 5 and 6 respectively). The M1 site occupancy is quite sensitive to the Ni distribution because of the well defined peak at 2.97 Å in the EXAFS model (shell 3, Table 4). This peak only involves backscattering of photoelectrons from central target Ni in M1 by Ni and Mg in an M1 outer shell. The errors in the EXAFS-refined Ni estimates in M1 are difficult to assess but might be about 10–15% relative for samples with $X_{Ni} = 0.2$ and 0.15 which show significant reductions in the *R* values following the Ni:Mg refinement for the M1 site (cf. columns 2 and 5, Table 5). The other samples show only small or no reductions in *R*-factors and errors are likely to be significantly higher; we have assumed relative errors of 20% for these samples. The M2 radial distribution is less well-defined than that for M1; refinement of the Ni:Mg ratio in the M2 site did not lead to further reduction of the *R*-factor and the occupancy values did not change significantly from the starting neutron data.

The EXAFS-refined Ni:Mg occupancies for samples with $X_{Ni} = 0.50$ and 0.80 are within error of the neutron values which is consistent with these samples lacking any short-range clustering of Ni and thus with their having homogeneous Ni:Mg

TABLE 5. Refinement of EXAFS to fit the ratios of Ni:Mg scatterers in M1

Sample	Refinement assuming complete homogeneity			Refinement of Ni:Mg in M1	
	R-factor	Ni:Mg in M1*	Ni:Mg in M2*	R-factor	Ni:Mg in M1
Mg _{1.7} Ni _{0.3} SiO ₄	31.1	0.26:0.74	0.04:0.96	30.9	0.60:0.40
Mg _{1.6} Ni _{0.4} SiO ₄	27.9	0.35:0.65	0.05:0.95	26.6	0.74:0.26
Mg _{1.5} Ni _{0.5} SiO ₄	38.4	0.42:0.58	0.08:0.92	36.4	0.75:0.25
Mg _{1.4} Ni _{0.6} SiO ₄	28.4	0.50:0.50	0.10:0.90	28.1	0.68:0.32
Mg _{1.0} Ni _{1.0} SiO ₄	41.9	0.73:0.27	0.27:0.73	41.9	0.68:0.32
Mg _{0.4} Ni _{1.6} SiO ₄	39.1	0.93:0.07	0.67:0.33	39.1	0.95:0.05

*Occupancies obtained at room temperature from neutron scattering.

occupancies in both M1 and M2 sites. By contrast, the four Mg-rich solid solutions all show significant enhancements in the proportions of Ni backscatterers in M1 sites over the values obtained by neutron diffraction for the bulk samples. These results reflect the clustering of Ni in adjacent M1 sites and point to the presence of Ni-rich domains in these samples and also that, in these domains, Ni tends to occupy M1 sites in preference to M2. The length scales of these domains are within the size range probed by XAS, and are likely to be an order of magnitude smaller in size than would be detectable by X-ray and neutron diffraction techniques. The implication is that the sample is a nanoscale two-phase mixture of components one of which has M1 sites substantially enriched in Ni relative to the bulk compositions, while the other must have M1 sites which are proportionately enriched in Mg. In addition, the four samples in the range $X_{Ni} = 0.30$ to 0.15 all show Ni-rich domain compositions with M1 Ni:Mg ratios within error of each other averaging about 0.68 ± 0.08 ; this value is within error of the M1 occupancy of the “homogeneous” MgNiSiO₄ sample. These results indicate the presence of an incipient solvus in the Mg-Ni olivine system with one end-member composition close to MgNiSiO₄ and the other with lower Ni contents than our most Mg-rich sample ($X_{Ni} = 0.15$). These relationships are shown in Figure 8; we have no evidence for the composition of the domains which have M1 sites enriched in Mg but we tentatively complete this part of the immiscibility loop assuming it to be more Mg-rich than the M2 sites for most of the bulk composition range (Fig. 8).

THERMODYNAMIC, KINETIC, AND CRYSTAL CHEMICAL IMPLICATIONS

Intersite exchange energies

We have shown that K_D values for both Ni-Mg samples from 800 to 1100 °C follow the same trend within error. The combined data sets when plotted on a van't Hoff diagram give an intersite exchange energy (ΔH_{ex}) of 21.5 ± 1.9 kJ/mol (Fig. 9); note that the exchange energy for Mg_{1.6}Ni_{0.4}SiO₄ alone is 22.1 ± 3.1 kJ/mol while that for MgNiSiO₄ is 20.5 ± 1.6 kJ/mol. Our estimate of 21.5 kJ/mol is in good agreement with the value of 19.5 kJ/mol deduced by Hirschmann (1992, 2000); both of these values contrast markedly with that of 12.5 kJ/mol (Hirschmann 1991). Our Ni-Mg cation exchange energy of 21.5 kJ/mol is distinctly higher than the values of 15.5 and 10.7 kJ/mol determined for MgMnSiO₄ and FeMnSiO₄ olivine, respectively (Henderson et al. 1996), and the value of about 11 kJ/mol estimated for MgFeSiO₄ olivine (Redfern et al. 2000). Note that these exchange energies compare with previously published ΔH_{ex} values of 15.8 kJ/mol for Mg-Mn, 11.8 kJ/mol for Fe-Mn, and 0 kJ/mol for Mg-Fe exchange (Hirschmann 1992; Hirschmann and Ghiorso 1994; Sack and Ghiorso 1989).

Akamatsu and Kumazara (1993) treated the kinetics of cation exchange between M1 and M2 sites as being equivalent to the cation interdiffusion rate along the *b* axis. Henderson et al. (1996) thus correlated the size of the M1-M2 site exchange energy with relative values for the atomic diffusion coefficients. The fact that the exchange energy for Mg-Ni is the highest for the olivines studied in our work is consistent with these corre-

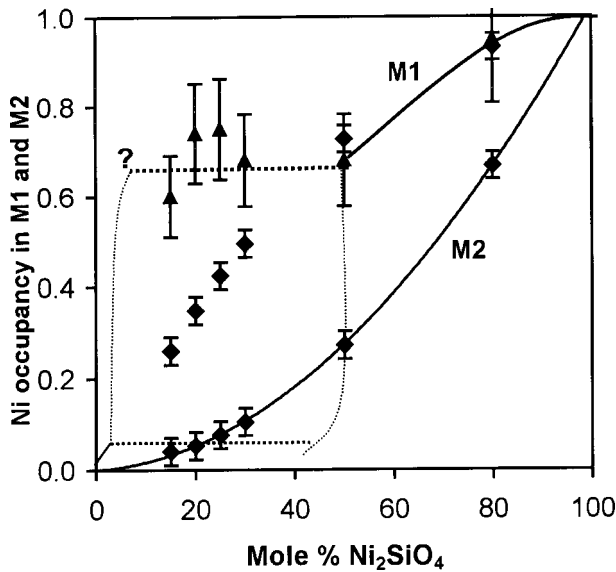


FIGURE 8. Variation of Ni site occupancy in the M1 and M2 sites at room T vs. bulk composition. Data obtained from neutron diffraction are shown as \blacklozenge while EXAFS data are shown as \blacktriangle . The four most Mg-rich samples all show clear evidence of Ni clustering in adjacent M1 sites pointing to the existence of two-phase behavior with a corresponding Mg-rich component. Note that the horizontal lines define the width of the immiscibility gap and the vertical lines show the hypothetical contrast in composition between the coexisting nano-scale phases. The dashed lines show the tentative geometry of this immiscibility "loop". The question mark is to show that the Mg-rich end of the immiscibility gap is unknown.

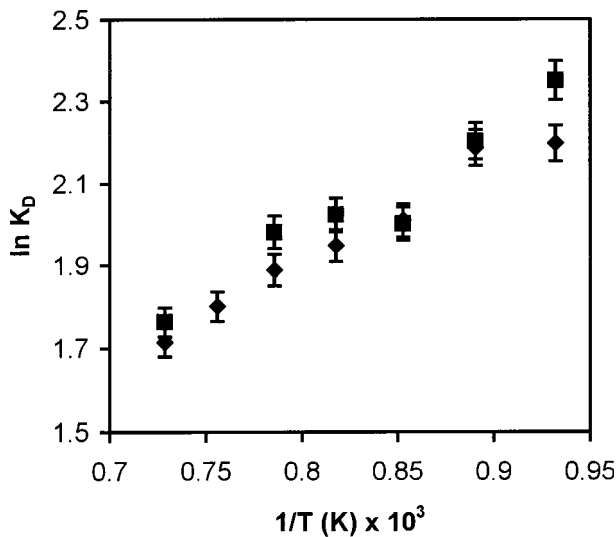


FIGURE 9. Van't Hoff K_D vs. $1/T$ (K) diagram for both samples at temperatures defining the equilibrium disordering trend (>800 °C). The slope of this trend gives a value for the ratio: intersite cation exchange energy/gas constant (R). Symbols: \blacksquare $\text{Mg}_{1.6}\text{Ni}_{0.4}\text{SiO}_4$; \blacklozenge $\text{Mg}_{1.0}\text{Ni}_{1.0}\text{SiO}_4$. 1σ error bars are shown.

lations as Ni has by far the smallest diffusion coefficient of 0.80×10^{-12} cm^2/s at 1200 °C, compared with values for Mn, Mg and Fe of 3.0 -, 6.0 -, and 48×10^{-12} cm^2/s (Miyamoto and Takeda 1983). The implication is that Ni-Mg exchange is likely to be slower than cation exchange between M1-M2 for the other olivine stoichiometries discussed here.

Activation energies and kinetic analysis

The order-disorder process in olivine is non-convergent, the two M sites always being symmetrically separate. Thus, a discrete cation order-disorder transition will fail to take place due to the chemical differences between sites that will distinguish them at all temperatures. Redfern et al. (1996, 1997) showed how the free energy of ordering and its time dependence can be modeled using a Landau approach. The non-convergent character can be described as an energy term, $-hQ$, that is linear in the order parameter. By adding such a term to the Landau expansion, one prevents $Q = 0$ from being a solution to $\partial\Delta G/\partial Q = 0$:

$$\Delta G(Q) = -hQ + \frac{a}{2}(T - T_c)Q^2 + \frac{b}{4}Q^4 + \dots \quad (1)$$

The equilibrium T -dependence of Q is given by the condition $\partial\Delta G/\partial Q = 0$. The T -dependent order-disorder data for both $\text{Mg}_{1.6}\text{Ni}_{0.4}\text{SiO}_4$ and MgNiSiO_4 have been fitted to this model for temperatures above 1000 K, the blocking temperature at which relaxation occurs on heating (Fig. 10). The parameters obtained are, for MgNiSiO_4 , $a/h = 0.00523$, $b/h = 13.4$, $T_c = 1330$ K, and for $\text{Mg}_{1.6}\text{Ni}_{0.4}\text{SiO}_4$, $a/h = 0.00683$, $b/h = 8.02$, $T_c = 1553$ K. These values are very similar to those for Fe-Mn and Mg-Mn olivines found by Redfern et al. (1996, 1997), although the values for T_c are higher. The ratio $h:aT_c$ is an indication of the relative strengths of the chemical potential difference between the two M sites, which forces non-convergent order, and the normal driving entropy of a convergent process (aT_c). In $\text{Mg}_{1.6}\text{Ni}_{0.4}\text{SiO}_4$ this ratio is 0.094 and in MgNiSiO_4 it is 0.144 . This compares with 0.174 for MgMnSiO_4 and 0.296 for FeMnSiO_4 (Redfern et al. 1997).

The kinetics of order-disorder at temperatures below 1000 K can be understood in terms of a straightforward extension of the Landau model. The essence of the theory is that the rate of change of ordering, dQ/dt , is dependent upon the probability of a jump towards the equilibrium state, and the rate of change of the free energy with order at the particular non-equilibrium state attained by the crystal. In the Ginzburg-Landau case the rate of change of order is given by:

$$\frac{dQ}{dt} = -\frac{\gamma \exp(-\Delta G^*/RT)}{2RT} \frac{\partial G}{\partial Q} \quad (2)$$

where γ is the characteristic effective jump frequency of the migrating atom and ΔG^* is the free energy of activation for the jump. The evolution of the order parameter can be understood in terms of its locus across a free energy surface as a function of time.

Integrating Equation 2 under isothermal conditions one obtains:

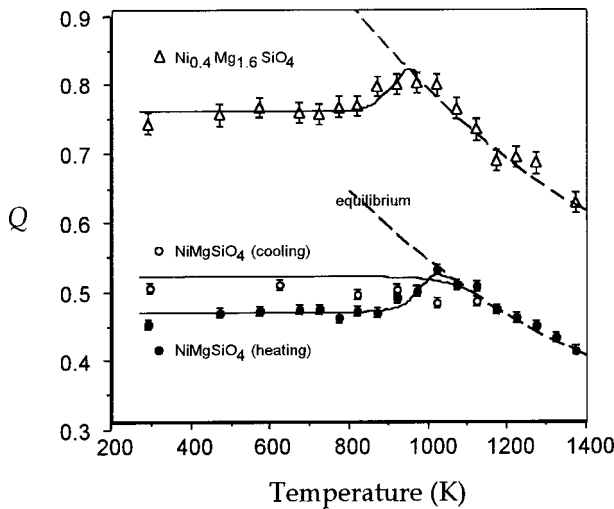


FIGURE 10. Variation of Q , the order parameter for Ni occupancy of M1, as a function of T . For NiMgSiO₄, solid samples are for heating runs and open symbols represent cooling data. The solid lines indicate the fit to the Ginzburg-Landau equation and the known heating and cooling rates. The dashed lines denote the high T equilibrium disordering behavior obtained from the Landau expression for free energy (Eq. 1).

$$t - t_0 = \int_{Q_0}^Q \frac{-2RT}{\gamma \exp(-\Delta G^*/RT) \left(\frac{\partial \Delta G}{\partial Q} \right)^{-1}} dQ \quad (3)$$

where Q_0 is the initial value of Q at time t_0 . This equation allows the time taken for a given change in Q to be calculated. Alternatively one may calculate the change in Q for a given annealing time by evaluating Equation 3 numerically, and varying the upper limit of integration in an iterative procedure until the correct annealing time is obtained. The evolution of Q vs. t during heating or cooling at a constant rate can be determined by approximating the constant heating or cooling rate by a series of discrete isothermal annealing steps separated by an instantaneous T change. The data for Mg_{1.6}Ni_{0.4}SiO₄ and MgNiSiO₄ at temperatures below that at which they reach equilibrium was analyzed in this manner to obtain an activation energy for order-disorder. This gives an activation energy for Ni-Mg exchange of 245 ± 5 kJ/mol for Mg_{1.6}Ni_{0.4}SiO₄ and 260 ± 5 kJ/mol for MgNiSiO₄. These values are higher than the values for Fe-Mn exchange and Mg-Mn exchange (193 and 172 kJ/mol respectively) quoted by Redfern et al. (1997). The magnitude of the activation energy influences the temperature at which relaxation towards equilibrium commences.

Using these results for Mg_{1.6}Ni_{0.4}SiO₄ olivine we can estimate the time-scale over which re-ordering occurs on heating a sample with an initial Q of 0.75 (as shown by our sample at room T). On shock heating such a sample to 673 K it would approach equilibrium by ordering. We have used Equation 3 to estimate the characteristic time-scale to get half-way towards the equilibrium value of Q ($t_{1/2}$) of such ordering. This follows a quasi-exponential rate law which on a $\ln(\text{time})$ vs. $1/T$ (K) defines a straight line of slope E/R (where E is activation energy and R is the gas constant). The results are displayed as

time (seconds) vs. T (°C) in Figure 11. The time taken to relax halfway to equilibrium at 400 °C is 20 years, which decreases to half an hour at 650 °C, and to around 2.5 min at 800 °C. At higher temperatures the sample would disorder, rather than order, on shock heating. Thus, for example, at 1000 °C $t_{1/2} = 2.5$ seconds while at 1300 °C $t_{1/2} = 0.03$ seconds. Based on these data, disordering experiments on Ni-Mg olivines involving annealing at 1300 °C (Ottonello et al. 1989; Boström 1989) would need to be cooled in a few milliseconds to prevent re-ordering on the quench. For example, using our cooling model, the K_D values for the three samples which Boström (1989) annealed at 1300 °C imply equilibrium temperatures of 1240, 1000, and 1040 °C for samples with $X_{\text{Ni}} = 0.30, 0.51$ and 0.76 , respectively. In effect, his three samples appear to have experienced significantly different cooling regimes (cf. Figure 2). The intersite exchange time-scale predicted by our model for 650–700 °C is consistent with the variations for Ni in M1 that were observed for refinements of our data obtained in 30 minute time-steps at these temperatures (see before).

This cooling model illustrates the extremely rapid ordering rates anticipated in olivines at geologically relevant temperatures, pointing to the inapplicability of inter-crystalline partitioning in olivines being used for the purpose of geothermometry. In addition, one would need rather rapid cooling rates at fairly low temperatures (below 600 °C) in order to quench-in non-equilibrium ordering patterns that might be treated as cooling rate indicators.

Our results can be used to shed further light on the observations of Ni-Mg order-disorder at high T and P in a NiMgSiO₄ olivine in the experiments of Chen et al. (1996). They heated a sample (held at 4 GPa) from room T to 800 °C over a time period of 40 minutes, and then held it for a further 69 minutes at 800 °C and 4 GPa. Initially, the sample showed a site occupancy of 0.742 Ni in M1. Taking this starting state, and calculating the expected time- T dependence of ordering for a similar sample held at 1 bar (using the model described above) we calculate the ordering pathway shown by the solid line in Fig-

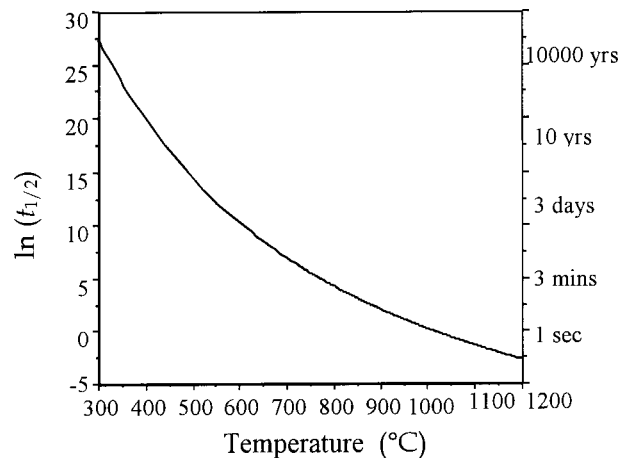


FIGURE 11. Cooling times to go half-way to the equilibrium value of Q ($t_{1/2}$) vs. time. This is an Arrhenius relationship which on a $\ln(\text{time})$ vs. $1/T$ (K) plot would give a straight line of slope E/R .

ure 12. It is clear that the degree of order observed by Chen et al. at times of 40 min and more is greater than that which we would expect for a sample held at 1 bar. Furthermore, their sample does not appear to have attained equilibrium order over the time scale of their experiment, while we would expect that a sample held at ambient P would reach equilibrium well within this time. This suggests that the effect of P on ordering in olivine is twofold. First, the effect is to increase the degree of order as predicted by Hazen and Navrotsky (1996) based on the common relationship that the volume of a disordered phase is larger than that of the equivalent ordered phase. We have noted that the distortion of the M1 site is crucial to its preferential occupation by Ni, which favors that site due to an increased crystal field stabilization. It seems that P increases the distortion of M1 over M2, increasing the tendency of Ni to partition into M1. Secondly, the kinetics of exchange between the two sites appear to be slower at 4 GPa than we would predict for a sample held at the same T but at one atmosphere P . This indicates that the activation volume of the exchange reaction is significant, and P makes the process more sluggish. This might also be expected, as the exchange is mediated through coupled exchange via the adjacent face-sharing and vacant octahedral sites; these sites are likely to have a greater compressibility than the fully occupied M1 and M2 sites, and therefore are likely to give rise to a substantial P -dependent activation energy. Following the approach of Hazen and Navrotsky (1996), using our data for the K_D values for NiMgSiO_4 at 800 °C and 1 bar and the extrapolated “equilibrium” value of Chen et al. (1996) at 800 °C and 4 GPa, implies a free energy change of about 1.54 kJ/mol. This value gives a volume of disordering ($\delta\Delta G_{\text{disorder}}/\delta P = \Delta V_{\text{disorder}}$)_T of 0.039 J/bar (0.39 cm³/mol), which is in excellent agreement with the value of 0.04 J/bar derived by Hazen and Navrotsky (1996) [based on the 1 bar Ni-Mg

olivine data of Ottonello et al. (1989)], and also with that of 0.035 ± 0.012 J/bar deduced by Hirschmann using data at 1 bar (1991, 1992).

Thermodynamic, crystal chemical, and D_{Ni} olivine/melt implications

Thermodynamic (macroscopic) measurements at elevated temperatures, and M1-M2 ordering effects in Ni-Mg olivine solid solutions have shown both positive and negative departures from ideality [i.e., the activity coefficient (γ) \neq 1.0]. Note that the formulation used by Bish (1981) for the cation-ordering-based (microscopic) activity of the Ni-olivine component in this system $\{a(\text{NiSiO}_{0.5}) = [(\theta_{\text{Ni}^{\text{M1}}}^{\text{M1}})(\theta_{\text{Ni}^{\text{M2}}}^{\text{M2}})]^{1/2}$, where θ represents fractional site occupancies} can only yield negative deviations from ideal, Raoult’s Law behavior. For analogous compositions, clear positive deviations from ideality have also been shown in thermodynamic experiments for Ni-Mn olivines (Huang et al. 1996) and Co-Mg olivines (Seifert and O’Neill 1987; Jacob et al. 1992), while Ni-Fe olivines show negative deviations (Ovchinnikov et al. 1992).

The experimental evidence described here for short-range Ni-Ni clustering in M1 is a clear indicator of non-ideality at the Mg-rich end of the solid solution series. The horizontal straight line shown in Figure 8 at a Ni content in M1 of 68% defines one limb of an immiscibility gap (solvus) between about MgNiSiO_4 and a Mg-rich end member between $X_{\text{Ni}} = 0.15$ and 0.00. This relationship is consistent with the thermodynamic results of Ottonello and Morlotti (1987) who found positive deviations from ideality which might suggest the presence of a solvus between about $X_{\text{Ni}} = 0.10$ and 0.60, and over a T range from about 1000 to 1200 °C. Further evidence for the non-ideal solution of Ni at low concentration (0.44 wt% NiO) in Mg-rich olivines is provided in Galois et al. (1995) who used Ni K-edge EXAFS to show that clusters between Ni in M1 and Fe in M2 tend to occur in a mantle olivine (Fo_{90}) from San Carlos, Arizona. Finally, our experimental results confirm the theoretical prediction of clustering in Mg-Ni olivines (Nikitina 1992; Ovchinnikov and Nikitina 1996). We conclude that our observation of short range Ni-Ni clustering in Mg-rich olivines confirms that the macroscopic indications that departures from ideality are positive rather than negative.

Fully disordered Ni-Mg solid solutions at room T might be expected to have unit-cell-parameters, and individual M-O bondlengths and O-M-O angles, falling on linear trends between the end members. Preferential ordering of Ni into the M1 site displaces Mg into M2 and, based on our M-O bond distances and O-M-O angular variance, it seems that the M2 polyhedron shows clear positive departures from such “ideal mixing” trends (Fig. 4). Although ordering of larger Mg into M2 might prevent a decrease in the b parameter with increasing Ni-content (making it independent of composition), the possible increase in b over the range $X_{\text{Ni}} = 0.00$ to 0.20 (Fig. 1) is difficult to rationalize. However, the presence of short range Ni clustering and sample immiscibility in the Mg-rich solid solutions might be responsible for the lattice distortions which produce the possible maximum in b (Fig. 1), and for the anomalously high M-O bond length values, for the $\text{Mg}_{1.6}\text{Ni}_{0.4}\text{SiO}_4$ sample (Fig. 4). A possible mechanism could be that these phe-

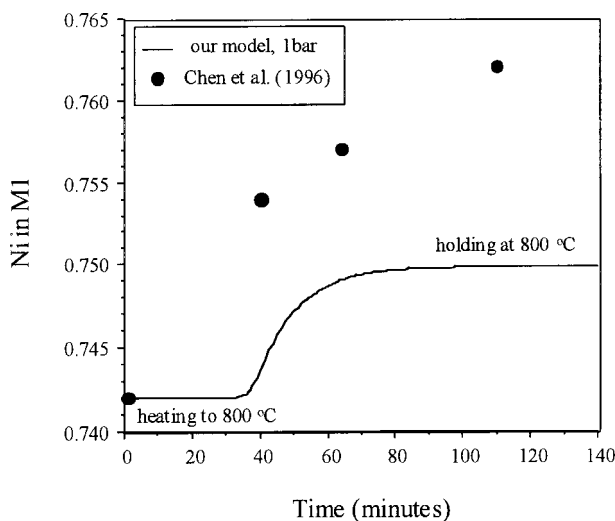


FIGURE 12. Comparison between the experimental ordering data determined by Chen et al. (1996) for MgNiSiO_4 olivine at elevated P (4 GPa) and T with data from our kinetic model for the same T conditions but at 1 atm pressure. The effect of P is to increase the degree of order and to slow down the M1-M2 intersite exchange rate.

nomena are related to elastic strains within the host matrix occurring at the interfaces between the immiscible nanoscale precipitates. A similar phenomenon is common in cryptoperthitic alkali feldspars where the *a* unit-cell parameter for the K-rich component has anomalously high values (Stewart and Wright 1974).

Experimental work carried out to determine the range of Ni concentration over which olivine/melt distribution coefficients for Ni (D_{Ni}) remained constant (i.e., Henry's Law obeyed) was the subject of much controversy some 20 years ago. To the best of our knowledge the discrepancies have never been satisfactorily explained. Mysen (1979, 1982) suggested that Henry's Law was not obeyed with over 1000 ppm Ni in olivine while other authors suggested that the upper limit was at least 6 wt% Ni (Drake and Holloway 1981) or even as high as 15 to 20 wt% Ni (e.g., Leeman and Lindstrom 1978). The upper values fall within the region of the immiscibility gap reported in this work and, although it seems unlikely, it is not impossible that some of the earlier melting experiments provided charges in which the Ni-rich components of a two-phase olivine mixture were analyzed preferentially. If there is any credence in this speculation, Mysen's 1000 ppm upper limit for Henry's Law behavior might represent the Mg-rich end of the immiscibility gap reported here.

ACKNOWLEDGMENTS

We thank NERC and CLRC for providing neutron and synchrotron beamtime and Jacques Barbier and an anonymous referee for their constructive comments. We also thank Nikita Ovchinnikov for sending reprints of their work published in Russia.

REFERENCES CITED

- Aikawa, N., Kumazawa, M., and Tokonami, M. (1985) Temperature dependence of intersite distribution of Mg and Fe in olivine and the associated change of lattice parameters. *Physics and Chemistry of Minerals*, 12, 1–8.
- Akamatsu, T., Fujino, K., Kumazawa, M., Fujimura, A., Kato, M., Sawamoto, H., and Yamanaka, T. (1988) Pressure and temperature dependence of cation distribution in Mg-Mn olivine. *Physics and Chemistry of Minerals*, 16, 105–113.
- Akamatsu, T., and Kumazawa, M. (1993) Kinetics of intracrystalline cation distribution in olivine and its implication. *Physics and Chemistry of Minerals*, 19, 423–430.
- Annersten, H., Ericsson, T., and Filippidis, A. (1982) Cation ordering in Ni-Fe olivines. *American Mineralogist*, 67, 1212–1217.
- Annersten, H., Adetunji, J., and Filippidis, A. (1984) Cation ordering in Fe-Mn silicate olivines. *American Mineralogist*, 69, 1110–1115.
- Ballet, O., Fuess, H., and Fritzsche, T. (1987) Magnetic structure and cation distribution in (Fe,Mn)₂SiO₄ (olivine) by neutron diffraction. *Physics and Chemistry of Minerals*, 15, 54–58.
- Binsted, N. (1998) EXCURV98—The Manual. CLRC Daresbury Laboratory Program.
- Bish, D.L. (1981) Cation ordering in synthetic and natural Ni-Mg olivine. *American Mineralogist*, 66, 770–776.
- Boström, D. (1987) Single-crystal X-ray diffraction studies of synthetic Ni-Mg olivine solid solutions. *American Mineralogist*, 72, 965–972.
- Boström, D. and Rosén, E. (1988) Determination of activity composition relations in (Ni,Mg)₂SiO₄ solid solutions at 1200–1600K by solid state emf measurements. *Acta Chemica Scandinavica*, 42, 149–155.
- Boström, D. (1989) Cation ordering at 1300°C in the (Ni,Mg)-olivine solid solution series. *Acta Chemica Scandinavica*, 43, 116–120.
- Brown, G.E. (1982) Olivines and silicate spinels. *Reviews in Mineralogy (Mineralogical Society of America)*, 5, 275–381.
- Campbell, F.E. and Roeder, P. (1968) The stability of olivine and pyroxene in the Ni-Mg-Si-O system. *American Mineralogist*, 53, 257–268.
- Cernik, R.J., Murray, P.K., Pattison, P., and Fitch, A.F. (1990) A two-circle powder diffractometer for synchrotron radiation with a closed loop encoder feedback system. *Journal of Applied Crystallography*, 23, 292–296.
- Chen, J., Li, R., Parise, J.B., and Weidner, D.J. (1996) Pressure-induced ordering in (Ni,Mg)₂SiO₄ olivine. *American Mineralogist*, 81, 1519–1522.
- Davies, P.K., and Navrotsky, A. (1981) Thermodynamics of solid solution formation in NiO-MgO and NiO-ZnO. *Journal of Solid State Chemistry*, 38, 264–276.
- de Waal, S.A. and Calk, L.C. (1973) Nickel minerals from Barberton, South Africa: VI. Liebenbergite, a nickel olivine. *American Mineralogist*, 58, 733–735.
- Della Giusta, A., Ottone, G., and Secco, L. (1990) Precision estimates of atomic distances using site occupancies, ionization potentials and polarizability in Pbmm silicate olivines. *Acta Crystallographica*, B46, 160–165.
- Drake, M.J. and Holloway, J.R. (1981) Partitioning of Ni between olivine and silicate melt: the "Henry's Law problem" reexamined. *Geochimica et Cosmochimica Acta*, 45, 431–439.
- Fleet, M.E. (1989) Activity coefficients for FeS and NiS in monosulfide liquid and NiSi_{0.5}O₂ in olivine from sulfide-silicate equilibria. *Geochimica et Cosmochimica Acta*, 53, 791–796.
- Fleet, M.E. (2000) Thermodynamics of multicomponent olivines and their solution properties of (Ni,Mg,Fe)₂SiO₄ and (Ca,Mg,Fe)₂SiO₄ olivines – Comment. *American Mineralogist*, 85, 1543–1547.
- Fujino, K., Sasaki, S., Takeuchi, Y., and Sadanaga, R. (1981) X-ray determination of electron distributions in forsterite, fayalite and tephroite. *Acta Crystallographica*, B37, 513–518.
- Galoisy, L., Calas, G., and Brown, G.E. (1995) Intracrystalline distribution of Ni in San Carlos olivine: an EXAFS study. *American Mineralogist*, 80, 1089–1092.
- Gurman, S.J., Binsted, N., and Ross, I. (1984) A rapid, exact curved-wave theory for EXAFS calculations. *Journal of Physics C – Solid State Physics*, 17, 143–151.
- Häkli, T.A. and Wright, T.L. (1967) The fractionation of nickel between olivine and augite as a geothermometer. *Geochimica et Cosmochimica Acta*, 31, 877–884.
- Hazen, R.M. (1976) Effects of temperature and pressure on the crystal structure of forsterite. *American Mineralogist*, 61, 1280–1293.
- Hazen, R.M., and Navrotsky, A. (1996) Effects of pressure on order-disorder reactions. *American Mineralogist*, 81, 1021–1035.
- Hedin, L. and Lundqvist, S. (1969) Effects of electron-electron and electron-phonon interactions on the one-electron state of solids. *Solid State Physics*, 23, 1–181.
- Henderson, C.M.B., Knight, K.S., Redfern, S.A.T., and Wood, B.J. (1996) High-temperature study of octahedral cation exchange in olivine by powder diffraction. *Science*, 271, 1713–1715.
- Henderson, P. and Dale, I.M. (1969) The partitioning of selected transition element ions between olivine and groundmass of oceanic basalts. *Chemical Geology*, 5, 267–274.
- Hirschmann, M. (1991) Thermodynamics of multicomponent olivines and the solution properties of (Ni,Mg,Fe)₂SiO₄ and (Ca,Mg,Fe)₂SiO₄ olivines. *American Mineralogist*, 76, 1232–1248.
- Hirschmann, M. (1992) Studies of nickel and minor elements in olivine and in silicate liquids. Ph.D. dissertation, University of Washington, Seattle, 166p.
- Hirschmann, M. and Ghiorso, M.S. (1994) Activities of nickel, cobalt, and manganese silicates in magmatic liquids and applications to olivine/liquid and to silicate/metal partitioning. *Geochimica et Cosmochimica Acta*, 58, 4109–4126.
- Hirschmann, M.M. (2000) Thermodynamics of multicomponent olivines and their solution properties of (Ni,Mg,Fe)₂SiO₄ and (Ca,Mg,Fe)₂SiO₄ olivines – Reply. *American Mineralogist*, 85, 1548–1555.
- Hu, X., Langer, K., and Böstrom, D. (1990) Polarized electronic absorption spectra and Ni-Mg partitioning in olivines (Mg_{1-x}Ni_x)₂[SiO₄]. *European Journal of Mineralogy*, 2, 29–41.
- Huang, J.-H., Böstrom, D., and Rosén, E. (1996) Phase relations and activities of (Mn,Ni)-olivine solid solution in the ternary system MnO-NiO-SiO₂. *Acta Chemica Scandinavica*, 50, 1102–1107.
- Jacob, K.T., Mukhopadhyay, S., and Shukla, A.K. (1992) *Journal of the American Ceramic Society*, 75, 3081–3086.
- Lee, P.A. and Pendry, J.B. (1975) Theory of extended X-ray absorption fine structure. *Physics Review*, B11, 2795–2811.
- Leeman, W.P. and Lindstrom, D.J. (1978) Partitioning of Ni²⁺ between basaltic and synthetic melts and olivines—an experimental study. *Geochimica et Cosmochimica Acta*, 42, 801–816.
- Lumpkin, G.R. and Ribbe, P.H. (1983) Composition, order-disorder and lattice parameters of olivines. I. Relationships in silicate, germanate, beryllate, phosphate and borate olivines. *American Mineralogist*, 68, 164–176.
- Matsui, Y. and Syono, Y. (1968) Unit-cell dimensions of some synthetic olivine group solid solutions. *Geochemical Journal*, 2, 51–59.
- Miyamoto, M. and Takeda, H. (1983) Atomic diffusion coefficients calculated for transition metals in olivine. *Nature*, 303, 602–603.
- Mysen, B.O. (1979) Nickel partitioning between olivine and silicate melt: Henry's law revisited. *American Mineralogist*, 64, 1107–1114.
- Mysen, B.O. (1982) Partitioning of Ni between olivine and silicate melt: the "Henry's Law problem" reexamined: discussion. *Geochimica et Cosmochimica Acta*, 46, 297–298.
- Nikitina, L.P. (1992) Short range ordering and thermodynamic properties of the (Mg_{1-x}Ni_x)₂SiO₄ solid solution with olivine structure. *Proceedings of the Russian Mineralogical Society*, 121(6), 10–20. [In Russian with English abstract]
- Nord, A.G., Annersten, H., and Filippidis, A. (1982) The cation distribution in synthetic Mg-Fe-Ni olivines. *American Mineralogist*, 67, 1206–1211.

- Ottoneo, G., Della Giusta, A., and Molin, G.M. (1989) Cation ordering in Ni-Mg olivines. *American Mineralogist*, 74, 411–421.
- Ottoneo, G. and Morlotti, R. (1987) Thermodynamics of the (nickel + magnesium) olivine solid solution. *Journal Chemical Thermodynamics*, 19, 809–818.
- Ottoneo, G., Princivalle, F., and Della Giusta, A. (1990) Temperature, composition and fO_2 effects on the intersite distribution of Mg and Fe^{2+} in olivines. *Physics and Chemistry of Minerals*, 17, 301–312.
- Ovchinnikov, N.O., Nikitina, L.P. and Khiltova, E.Yu. (1992) The real structure and thermodynamic properties of olivine solid solutions ($Fe_{1-x}Ni_x$)₂SiO₄. *Proceedings of the Russian Mineralogical Society*, 121(4), 15–28. [In Russian with English abstract]
- Ovchinnikov, N.O., and Nikitina, L.P. (1996) Crystallochemistry of ordering and thermodynamic properties of Ni-bearing olivines on the basis of fayalite and forsterite. *Proceedings of the Russian Mineralogical Society*, 125(6), 49–28. [In Russian with English abstract]
- Princivalle, F. (1990) Influence of temperature and composition on Mg- Fe^{2+} of natural olivines. *Mineralogy and Petrology*, 43, 121–129.
- Rager, H., Hosoya, S., and Weiser, G. (1988) Electron-paramagnetic resonance and polarized optical absorption spectra of Ni^{2+} in synthetic forsterite. *Physics and Chemistry of Minerals*, 15, 383–389.
- Rajamani, V., Brown, G.E., and Prewitt, C.T. (1975) Cation ordering in Ni-Mg olivine. *American Mineralogist*, 60, 292–299.
- Redfern, S.A.T., Henderson, C.M.B., Wood, B.J., Harrison, R.J., and Knight, K.S. (1996) Determination of olivine cooling rates from metal-cation ordering. *Nature*, 381, 407–409.
- Redfern, S.A.T., Henderson, C.M.B., Knight, K.S., and Wood, B.J. (1997) High-temperature order-disorder in ($Fe_{0.5}Mn_{0.5}$)₂SiO₄ and ($Mn_{0.5}Mg_{0.5}$)₂SiO₄ olivines: an *in situ* neutron diffraction study. *European Journal of Mineralogy*, 9, 287–300.
- Redfern, S.A.T., Knight, K.S., Henderson, C.M.B., and Wood, B.J. (1998) Fe-Mn ordering in fayalite-tephroite (Fe_xMn_{1-x})₂SiO₄ olivines: a neutron diffraction study. *Mineralogical Magazine*, 62, 607–615.
- Redfern, S.A.T., Artioli, G., Rinaldi, R., Henderson, C.M.B., Knight, K.S., and Wood, B.J. (2000) High-temperature octahedral cation ordering in synthetic MgFeSiO₄ olivine: an *in situ* neutron powder diffraction study. *Physics and Chemistry of Minerals*, 27, 630–637.
- Rietveld, H.M. (1968) A profile refinement method for nuclear and magnetic structures. *Journal of Applied Crystallography*, 2, 65–71.
- Ringwood, A.E., and Major, A. (1966) Synthesis of Mg₂SiO₄-Fe₂SiO₄ solid solutions. *Earth and Planetary Science Letters*, 1, 241–245.
- Robinson, K., Gibbs, G.V., and Ribbe, P.H. (1971) Quadratic elongation: a quantitative measure of distortion in coordination polyhedra. *Science*, 172, 567–570.
- Sack, R.O. and Ghiorso, M.S. (1989) Importance of considerations of mixing properties in establishing an internally consistent thermodynamic database: Thermochemistry of minerals in the system Mg₂SiO₄-Fe₂SiO₄-SiO₂. *Contributions to Mineralogy and Petrology*, 102, 41–68.
- Seifert, S. and O'Neill, H. St J. (1987) Experimental determination of activity-composition relations in Ni₂SiO₄-Mg₂SiO₄ and Co₂SiO₄-Mg₂SiO₄ olivine solid solutions at 1200K and 0.1MPa and 1573 K and 0.5 GPa. *Geochimica et Cosmochimica Acta*, 51, 97–104.
- Snyder, J.G. (1993) High-temperature cation ordering in nickel-magnesium olivine. M.Sc. Thesis Queen's University, Kingston, Ontario, Canada. 88p.
- Stewart, D.B. and Wright, T.L. (1974) Al/Si order and symmetry of natural alkali feldspars, and the relationship of strained cell parameters to bulk composition. *Bulletin de la Société française de Minéralogie et de Cristallographie*, 97, 356–377.
- Tsukimura, K. and Sasaki, S. (2000) Determination of cation distribution in (Co,Ni,Zn)₂SiO₄ olivine by synchrotron X-ray diffraction. *Physics and Chemistry of Minerals*, 27, 234–241.
- Vokurka, K. and Rieder, M. (1987) Thermal expansion and excess volumes of synthetic olivines on the Mg₂SiO₄-Ni₂SiO₄ join. *Neues Jahrbuch für Mineralogie Monatshefte*, H3, 97–106.
- Wood, B.J. (1974) Crystal field spectra of Ni^{2+} in olivine. *American Mineralogist*, 59, 244–248.

MANUSCRIPT RECEIVED SEPTEMBER 27, 2000

MANUSCRIPT ACCEPTED JUNE 11, 2001

MANUSCRIPT HANDLED BY MICHAEL E. FLEET